Asymptotic analysis of small defects near a singular point in anti-plane elasticity. Application to the nucleation of a crack at a notch

Thi Bach Tuyet Dang, Laurence Halpern, Jean-Jacques Marigo

MEMOCS
Volume 00 (Pages 000–000)

ASYMPTOTIC ANALYSIS OF SMALL DEFECTS NEAR A SINGULAR POINT IN ANTI-PLANE ELASTICITY. APPLICATION TO THE NUCLEATION OF A CRACK AT A NOTCH.

Thi Bach Tuyet Dang, Laurence Halpern, and Jean-Jacques Marigo

Abstract. We use matching asymptotic expansions to treat the anti-plane elastic problem associated with a small defect located at the tip of a notch. In a first part, we develop the asymptotic method for any type of defect and present the sequential procedure which allows us to calculate the different terms of the inner and outer expansions at any order. That requires in particular to separate in each term its singular part from its regular part. In a second part, the asymptotic method is applied to the case of a crack of variable length located at the tip of a given notch. We show that the first two non trivial terms of the expansion of the energy release rate are sufficient to well approximate the dependence of the energy release rate on the crack length in the range of values of the length which are sufficient to treat the problem of nucleation. This problem is considered in the last part where we compare the nucleation and the propagation of a crack predicted by two different models: the classical Griffith law and the Francfort-Marigo law based on an energy minimization principle. Several numerical results illustrate the interest of the method.

1. Introduction

A major issue in fracture mechanics is how to model the initiation of a crack in a sound material, see [7]. There are two difficulties: the first one is to propose a law able to predict that nucleation; the second is a purely numerical issue. Indeed, it is difficult to compute with a good accuracy the energy release rate associated with a crack of small length which appears at the tip of a notch, see [33]. The classical finite element method leads to inaccurate results because of the overlap of two singularities which cannot be correctly captured by this method: one is due to the tip of the notch, the other is due to the tip of the crack. A specific method of approximation based on asymptotic expansions is preferable as it is developed in analogous situations with localized defects, see for instance [1, 2, 4, 5, 6, 16, 23, 32, 34, 40]. The first part of the present paper is devoted to the presentation of this Matched Asymptotic Method (shortly, the MAM) in the case of a defect (which includes the case of a crack) located at the tip of a notch in the simplified context of antiplane linear elasticity. Therefore, our approach can be considered as a particular case of the previous works which have been devoted to the study of elliptic problems in corner domains, like [14, 15, 26, 27]. However, a major difference is that we want to use these asymptotic methods to predict the nucleation or the propagation of defects (like cracks) near those singular points. The second and third parts of our paper will be devoted to this task. That requires, of course, to introduce a criterion of nucleation. This delicate issue has not received a definitive answer at the present time and it was considered for a long time as a problem which could not be solved in the framework of Griffith theory of fracture [8, 13, 30, 31]. The main invoked reason is that the release of energy due to a small crack tends to zero when the length of the crack tends to zero, see [11, 33]. Therefore, according to the Griffith criterion which stands that the crack can propagate only when the energy release rate reaches a

Date: Submitted, 18 december 2012.
2000 *Mathematics Subject Classification.* 35A15, 35B40, 74A45, 74G70, 74R10.
Key words and phrases. Brittle fracture, variational methods, asymptotic methods, singularities.
This work was partially supported by the French Agence Nationale de la Recherche (ANR), under grant epsilon (BLAN08-2_312370) "Domain decomposition and multi-scale computations of singularities in mechanical structures".

critical value characteristic of the material, no nucleation is possible because the energy release rate vanishes when there is no preexisting crack. This limitation of Griffith's theory was one of the motivations which lead Francfort and Marigo in [22] to replace the Griffith criterion by a principle of least energy, in the spirit of the original idea of Griffith [25]. It turns out that the principle of least energy is really able to predict the nucleation of cracks in a sound body. However, as it was generically proved in [11, 22], the nucleation is necessarily brutal in the sense that a crack of finite length suddenly appears at a critical loading. Accordingly, we propose to revisit the problem of nucleation of a crack at the tip of a notch by comparing the two criteria. One of our goal is to use the MAM to obtain semi-analytical expressions for the critical loading at which a crack appears and the length of the nucleated crack.

Specifically, the paper is organized as follows. Section 2 is devoted to the description of the MAM on a generic anti-plane linear elastic problem where the body contains a defect near the tip of a notch. We first decompose the solution into two expansions: the *outer expansion* is valid far enough from the tip of the notch while the *inner expansion* is valid in a neighborhood of the tip of the notch. These expansions contain a sequence of inner and outer terms which are solutions of inner and outer problems and are connected by the matching conditions. Moreover each term contains a regular and a singular part. We explain how all the terms and the coefficients entering in their singular and regular parts are sequentially determined. The section finishes by an example where the exact solution is obtained in closed form and hence where we can verify the relevance of the MAM.

In Section 3, the MAM is applied to the case where the defect is a crack. Its main goal is to compute with a good accuracy the energy release rate associated with a crack of small length near the tip of the notch. Indeed, it is a real issue in the case of a genuine notch (by opposition to a crack) because the energy release rate starts from 0 when the length of the nucleated crack is 0, then is rapidly increasing with the length of the crack before reaching a maximum and is finally decreasing. Accordingly, after the setting of the problem, the computation of the energy release rate by the FEM is described, and the reason why the numerical results are less accurate when the crack length is small is given. Then, the MAM is used to compute the energy release rate for small values of the crack length. As expected, the computation shows that, the smaller the size of the defect, the more accurate is the approximation by the MAM at a certain order. It even appears that very accurate results can be obtained by computing a small number of terms in the matched asymptotic expansions. We discuss also the influence of the angle of the notch on the accuracy of the results, this angle playing an important role in the process of nucleation (because, in particular, the length ℓ_{m} at which the maximum of the energy release rate is reached depends on the angle of the notch). It turns out that when the notch is sufficiently sharp, *i.e.* sufficiently close to a crack, the first two non trivial terms of the expansion of the energy release rate are sufficient to capture with a very good accuracy the dependence of the energy release rate on the crack length.

In section 4, we study the problem of crack nucleation at the tip of a notch. We first introduce the two competing evolution laws, *i.e.* the *G-law* and the *FM-law*: the first one is the usual Griffith's law based on the criterion of critical energy release rate, the second is that introduced in [22] and which is based on the concept of energy minimization. We recall some general results previously established in [33] and extend them to the present case of a notch-shaped body in an antiplane setting. By virtue of the good approximation given by the MAM, we are able to solve the evolution problem in a quasi closed form, the solution depending only on two coefficients that must be computed by the FEM. That permits a qualitative and quantitative comparison of the two laws.

2. The real problem and its expansion by the Matched Asymptotic Method

2.1. **The real problem.** Here, we consider a small geometrical defect of size ℓ (like a crack or a void) located near the corner of a notch, see Figure 1. The geometry of the notch is characterized by its angle ω, see Figure 2. The tip of the notch is taken as the origin of the space. We will introduce two scales of coordinates: the "macroscopic" coordinates $\mathbf{x} = (x_1, x_2)$ used in the outer domain, and the "microscopic" coordinates $\mathbf{y} = \mathbf{x}/\ell = (y_1, y_2)$ used in the neighborhood of the tip of the notch where the defect is located, see Figure 2. In the case of a crack, the axis x_1 is chosen in such a way that the crack corresponds to the line segment $(0, \ell)\times\{0\}$. The unit vector orthogonal to the (x_1, x_2) plane is denoted by $\mathbf{e}_3$.

The natural reference configuration of the *sound* two-dimensional body is Ω_0 while the associated body which contains a defect of size ℓ is Ω_ℓ. The part of the boundary of Ω_ℓ which is due to the defect is denoted by Γ_ℓ, *i.e.*

$$\Gamma_\ell = \partial\Omega_\ell \setminus \partial\Omega_0, \tag{1}$$

Γ_ℓ is contained in the disk of center $(0, 0)$ and radius ℓ. In the case of a crack, Γ_ℓ is the crack itself, *i.e.* $\Gamma_\ell = (0, \ell)\times\{0\}$. The two edges of the notch are denoted by Γ^+ and Γ^-. To simplify the presentation, it is assumed that they are not modified by the introduction of the defect, see Figure 1. When using polar coordinates (r, θ), the pole is the tip of the notch and the origin of the polar angle is the edge Γ^-. Accordingly, we have

$$r = |\mathbf{x}|, \quad \Gamma^- = \{(r, \theta), 0 < r < r^*, \quad \theta = 0\}, \qquad \Gamma^+ = \{(r, \theta), 0 < r < r^*, \quad \theta = \omega\}. \tag{2}$$

This body is made of an elastic isotropic material whose shear modulus is $\mu > 0$. It is submitted to a loading such that the displacement field at equilibrium $\mathbf{u}_\ell$ be antiplane, *i.e.*

$$\mathbf{u}_\ell(\mathbf{x}) = u_\ell(x_1, x_2)\mathbf{e}_3$$

where the subscript letter ℓ is used in order to recall that the real displacement depends on the size of the defect. We assume that the body forces are zero and then u_ℓ must be an harmonic function in order to satisfy the equilibrium equations in the bulk:

$$\Delta u_\ell = 0 \quad \text{in} \quad \Omega_\ell. \tag{3}$$

The edges of the notch are free while Γ_ℓ is submitted to a density of (antiplane) surface forces. Accordingly, the boundary conditions on Γ_ℓ and $\Gamma^\pm$ are

$$\frac{\partial u_\ell}{\partial \nu} = 0 \quad \text{on} \quad \Gamma^\pm, \qquad \frac{\partial u_\ell}{\partial \nu}(\mathbf{x}) = \frac{g(\mathbf{y})}{\ell} \quad \text{on} \quad \Gamma_\ell. \tag{4}$$

In (4), ν denotes the unit outer normal vector to Ω_ℓ, and we assume that the density of (antiplane) surface forces depends on the microscopic variable $\mathbf{y}$ and has a magnitude of the order of $1/\ell$.

The remaining part of the boundary of Ω_ℓ is divided into two parts: Γ_D where the displacement is prescribed and Γ_N where (antiplane) surface forces are prescribed. Specifically, we have

$$u_\ell = f \quad \text{on} \quad \Gamma_D, \qquad \frac{\partial u_\ell}{\partial \nu} = h \quad \text{on} \quad \Gamma_N. \tag{5}$$

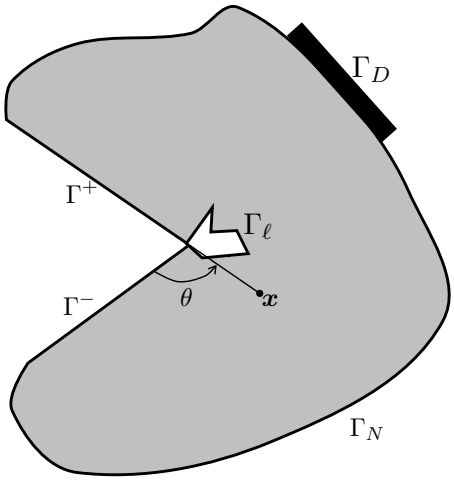

FIGURE 1. The domain Ω_ℓ for the real problem

The following proposition is a characterization of those functions which are harmonic in an angular sector and whose normal derivatives vanish on the edges of the sector. It is of constant use throughout the paper.

Proposition 1. *Let r_1 and r_2 be such that $0 \le r_1 < r_2 \le +\infty$ and let $\mathcal{D}_{r_1}^{r_2}$ be the angular sector*

$$\mathcal{D}_{r_1}^{r_2} = \{(r,\theta) \ : \ r \in (r_1, r_2), \quad \theta \in (0,\omega)\}.$$

Then any function u which is harmonic in $\mathcal{D}_{r_1}^{r_2}$ and which satisfies the Neumann condition $\partial u/\partial\theta = 0$ on the sides $\theta = 0$ and $\theta = \omega$ can be expanded as

$$u(r,\theta) = \mathsf{a}_0 \ln(r) + \mathsf{d}_0 + \sum_{n\in\mathbb{N}^*} \left(\mathsf{a}_n r^{-n\lambda} + \mathsf{d}_n r^{n\lambda}\right) \cos(n\lambda\theta), \quad \lambda = \frac{\pi}{\omega} \tag{6}$$

where the a_n and the d_n constitute two sequences of real numbers which are characteristic of u.

PROOF. Since the normal derivative vanishes at $\theta = 0$ and $\theta = \omega$, $u(r,\theta)$ can be expanded in Fourier series as:

$$u(r,\theta) = \sum_{n\in\mathbb{N}} f_n(r) \cos(n\lambda\theta).$$

In order that u be harmonic, the functions f_n must satisfy $r^2 f_n'' + r f_n' - n^2\lambda^2 f_n = 0$, for each n. We easily deduce that $f_0(r) = \mathsf{a}_0 \ln(r) + \mathsf{d}_0$ and $f_n(r) = \mathsf{a}_n r^{-n\lambda} + \mathsf{d}_n r^{n\lambda}$ for $n \ge 1$. □

2.2. **The matching asymptotic method (MAM).** We will write two asymptotic expansions of u_ℓ in terms of the small parameter ℓ. The inner expansion is valid in the neighborhood of the tip of the notch, while the the outer expansion, is valid far from this tip. These two expansions will be matched in an intermediate zone.

2.2.1. *The outer expansion.* Far from the tip of the notch, *i.e.* for $r \gg \ell$, u_ℓ does not see the notch, and we assume that it can be expanded as

$$u_\ell(\mathbf{x}) = \sum_{i\in\mathbb{N}} \ell^{i\lambda} u^i(\mathbf{x}). \tag{7}$$

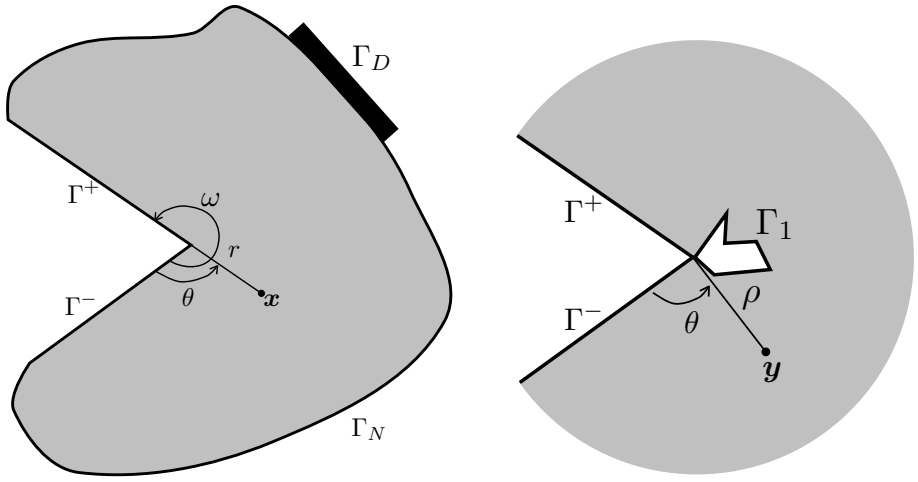

FIGURE 2. The domains Ω_0 and Ω^∞ for, respectively, the outer (left) and the inner (right) problems

In (7), even if this expansion is valid far enough from $r = 0$ only, u^i must be defined in the whole outer domain Ω_0 which corresponds to the sound body, see Figure 2-left. Inserting this expansion into (3,4,5) yields the sequence of problems for the u^i:

The first outer problem $i = 0$:

$$\begin{cases} \Delta u^0 = 0 & \text{in } \Omega^0 \\ \dfrac{\partial u^0}{\partial \nu} = 0 & \text{on } \Gamma^+ \cup \Gamma^- \\ \dfrac{\partial u^0}{\partial \nu} = h(\mathbf{x}) & \text{on } \Gamma_N \\ u^0 = f(\mathbf{x}) & \text{on } \Gamma_D \end{cases} \tag{8}$$

The other outer problems $i \geq 1$:

$$\begin{cases} \Delta u^i = 0 & \text{in } \Omega^0 \\ \dfrac{\partial u^i}{\partial \nu} = 0 & \text{on } \Gamma^+ \cup \Gamma^- \\ \dfrac{\partial u^i}{\partial \nu} = 0 & \text{on } \Gamma_N \\ u^i = 0 & \text{on } \Gamma_D \end{cases} \tag{9}$$

Moreover, the behavior of u^i in the neighborhood of $r = 0$ is singular and the singularity will be given by the matching conditions.

2.2.2. *The inner expansion.* Near the tip of the notch, *i.e.* for $r \ll 1$, we assume that the displacement field u_ℓ can be expanded as

$$u_\ell(\mathbf{x}) = \ln(\ell) \sum_{i \in \mathbb{N}} \ell^{i\lambda} w^i(\mathbf{y}) + \sum_{i \in \mathbb{N}} \ell^{i\lambda} v^i(\mathbf{y}), \qquad \mathbf{y} = \frac{\mathbf{x}}{\ell}. \tag{10}$$

In (10), even if this expansion is valid only in the neighborhood of $r = 0$, the fields v^i and w^i must be defined in the infinite inner domain Ω^∞. The domain Ω^∞ is the infinite angular sector $\mathcal{D}_0^\infty$ of the (y_1, y_2) plane, from which the rescaled defect of size 1 is removed, see Figure 2-right. Accordingly, the rescaled boundary Γ_1 of the defect is

$$\Gamma_1 = \partial\Omega^\infty \setminus \partial\mathcal{D}_0^\infty. \tag{11}$$

(In the case of a crack, $\Gamma_1 = (0, 1) \times \{0\}$.) Inserting this expansion into the set of equations constituting the real problem yields the sequence of problems for the v^i:

The first inner problem $i = 0$

$$\begin{cases} \Delta v^0 = 0 & \text{in } \Omega^\infty \\ \dfrac{\partial v^0}{\partial \theta} = 0 & \text{on } \theta = 0 \text{ and } \theta = \omega \\ \dfrac{\partial v^0}{\partial \nu} = g(\mathbf{y}) & \text{on } \Gamma_1 \end{cases} \tag{12}$$

The other inner problems $i \geq 1$

$$\begin{cases} \Delta v^i = 0 & \text{in } \Omega^\infty \\ \dfrac{\partial v^i}{\partial \theta} = 0 & \text{on } \theta = 0 \text{ and } \theta = \omega \\ \dfrac{\partial v^i}{\partial \nu} = 0 & \text{on } \Gamma_1 \end{cases} \tag{13}$$

The w^i must satisfy, for every $i \geq 0$ the same equations as the v^i for $i \geq 1$. To complement the set of equations, the behavior at infinity of the v^i and the w^i must be added. It is obtained by the matching conditions from the outer problems.

2.2.3. *Matching conditions.* In any sector $\mathcal{D}_0^{r_2}$ with $\ell \ll r_2 \ll 1$, the displacement fields u^i in the outer expansion are harmonic and satisfy homogeneous Neumann boundary conditions on the edges. Therefore Proposition 1 applies, and

$$u^i(\mathbf{x}) = \mathsf{a}_0^i \ln(r) + \mathsf{d}_0^i + \sum_{n\in\mathbb{N}^*} \left(\mathsf{a}_n^i r^{-n\lambda} + \mathsf{d}_n^i r^{n\lambda} \right) \cos(n\lambda\theta). \tag{14}$$

As for the inner expansion, the displacement fields v^i and w^i are harmonic in the sector $\mathcal{D}_1^\infty$ of the $\mathbf{y}$ plane and satisfy homogeneous Neumann boundary conditions on the edges. Therefore Proposition 1 applies, with the microscopic coordinates $\mathbf{y}$ and $\rho = |\mathbf{y}| = r/\ell$ replacing the macroscopic coordinates $\mathbf{x}$ and r:

$$v^i(\mathbf{y}) = \mathsf{c}_0^i \ln(\rho) + \mathsf{b}_0^i + \sum_{n\in\mathbb{N}^*} \left(\mathsf{c}_n^i \rho^{-n\lambda} + \mathsf{b}_n^i \rho^{n\lambda} \right) \cos(n\lambda\theta), \tag{15}$$

$$w^i(\mathbf{y}) = \mathsf{e}_0^i \ln(\rho) + \mathsf{f}_0^i + \sum_{n\in\mathbb{N}^*} \left(\mathsf{e}_n^i \rho^{-n\lambda} + \mathsf{f}_n^i \rho^{n\lambda} \right) \cos(n\lambda\theta). \tag{16}$$

The outer expansion and the inner expansion are both valid in any intermediate zone $\mathcal{D}_{r_1}^{r_2}$ such that $\ell \ll r_1 < r_2 \ll 1$. Inserting (14) into the outer expansion (7) with $r = \ell\rho$ leads to

$$u_\ell(\mathbf{x}) = \sum_{i\in\mathbb{N}} \ln(\ell)\ell^{i\lambda} \mathsf{a}_0^i + \sum_{i\in\mathbb{N}} \ell^{i\lambda} \Big(\mathsf{a}_0^i \ln(\rho) + \mathsf{d}_0^i + \sum_{n\in\mathbb{N}^*} \left(\mathsf{a}_n^{i+n} \rho^{-n\lambda} + \mathsf{d}_n^{i-n} \rho^{n\lambda} \right) \cos(n\lambda\theta) \Big), \tag{17}$$

with the convention that $\mathsf{d}_n^{i-n} = 0$ when $n > i$. Inserting (15) and (16) into the inner expansion (10) leads to

$$\begin{aligned} u_\ell(\mathbf{x}) &= \sum_{i\in\mathbb{N}} \ln(\ell)\ell^{i\lambda} \Big(\mathsf{e}_0^i \ln(\rho) + \mathsf{f}_0^i + \sum_{n\in\mathbb{N}^*} \left(\mathsf{e}_n^i \rho^{-n\lambda} + \mathsf{f}_n^i \rho^{n\lambda} \right) \cos(n\lambda\theta) \Big) \\ &+ \sum_{i\in\mathbb{N}} \ell^{i\lambda} \Big(\mathsf{c}_0^i \ln(\rho) + \mathsf{b}_0^i + \sum_{n\in\mathbb{N}^*} \left(\mathsf{c}_n^i \rho^{-n\lambda} + \mathsf{b}_n^i \rho^{n\lambda} \right) \cos(n\lambda\theta) \Big). \end{aligned} \tag{18}$$

Both expansions (17) and (18) are valid provided that $1 \ll \rho \ll 1/\ell$. Identification of these expansions provides the connections between the coefficients of the inner and outer expansions decribed in Table 1.

Remark 1. *From Table 1 can be deduced that the fields w^i are constant in the whole inner domain:*

$$w^i(\mathbf{y}) = \mathsf{a}_0^i, \qquad \forall \mathbf{y} \in \Omega^\infty, \quad \forall i \geq 0. \tag{19}$$

Therefore, these fields will be determined once the constants a_0^i will be known.

$\mathsf{e}_n^i = 0$	$i \geq 0,\, n \geq 0$
$\mathsf{f}_0^i = \mathsf{a}_0^i$	$i \geq 0$
$\mathsf{f}_n^i = 0$	$i \geq 0,\ n \geq 1$
$\mathsf{a}_n^i = 0$	$n > i \geq 0$
$\mathsf{c}_n^i = \mathsf{a}_n^{i+n}$	$i \geq 0,\, n \geq 0$
$\mathsf{b}_n^i = 0$	$n > i \geq 0$
$\mathsf{d}_n^i = \mathsf{b}_n^{i+n}$	$i \geq 0,\, n \geq 0$

TABLE 1. The relations between the coefficients of the inner and outer expansions given by the matching conditions

2.2.4. *The singular behavior of the u^i and the v^i.* On the matching conditions can be read the behavior of u^i in the neighborhood of $r = 0$ and the behavior of v^i at infinity. In particular, the form of their singularities is visible, according to the following definition.

Definition 1. *A field u defined in Ω_0 is* regular *in Ω_0 if $u \in H^1(\Omega_0)$, i.e. $u \in L^2(\Omega_0)$ and $\nabla u \in L^2(\Omega_0)^2$. It is* singular *otherwise.*

A field u defined in the unbounded domain Ω^∞ is regular *in Ω^∞ if $\nabla u \in (L^2(\Omega^\infty))^2$ and $\lim_{\rho\to\infty} u(\rho,\theta) = 0$. It is* singular *otherwise.*

Remark 2. *In other words, a field is regular if the associated elastic energy is finite. It is singular otherwise. In the case of the unbounded domain Ω^∞, a constant field is with finite energy, but the condition at infinity is added in order to fix the constant and obtain the uniqueness in the forthcoming boundary value problems.*

According to the analysis in the previous subsection, the field u^0 can be expanded in a neighborhood of the tip of the notch as

$$u^0(\mathbf{x}) = \mathsf{a}_0^0 \ln(r) + \sum_{n\in\mathbb{N}} \mathsf{b}_n^n r^{n\lambda}\cos(n\lambda\theta). \tag{20}$$

In the domain Ω_0, $\ln(r)$ is singular whereas $r^{n\lambda}\cos(n\lambda\theta)$ is regular for $n \geq 0$, in the sense of Definition 1. Accordingly, u^0 is split into into its singular and regular part as follows:

$$u^0(\mathbf{x}) = u_S^0(\mathbf{x}) + \bar{u}^0(\mathbf{x}), \tag{21}$$

$$u_S^0(\mathbf{x}) = \mathsf{a}_0^0 \ln(r), \quad \bar{u}^0 \in H^1(\Omega_0). \tag{22}$$

In the same way, for $i \geq 1$, the field u^i can be expanded in a neighborhood of the tip of the notch as

$$u^i(\mathbf{x}) = \mathsf{a}_0^i \ln(r) + \sum_{n=1}^{i} \mathsf{a}_n^i r^{-n\lambda}\cos(n\lambda\theta) + \sum_{n\in\mathbb{N}} \mathsf{b}_n^{i+n} r^{n\lambda}\cos(n\lambda\theta). \tag{23}$$

Since $r^{-n\lambda}\cos(n\lambda\theta)$ is singular (for $n \geq 0$) in the sense of Definition 1, u^i is split into its singular and regular part as follows:

$$u^i(\mathbf{x}) = u_S^i(\mathbf{x}) + \bar{u}^i(\mathbf{x}), \tag{24}$$

$$u_S^i(\mathbf{x}) = \mathsf{a}_0^i \ln(r) + \sum_{n=1}^{i} \mathsf{a}_n^i r^{-n\lambda}\cos(n\lambda\theta), \quad \bar{u}^i \in H^1(\Omega_0). \tag{25}$$

For the fields v^i of the inner expansion, the behavior at infinity comes into play. By virtue of the analysis in the previous subsection, the field v^i for $i \geq 0$ can be expanded for large ρ as

$$v^i(\mathbf{y}) = \mathsf{a}_0^i \ln(\rho) + \sum_{n=0}^{i} \mathsf{b}_n^i \rho^{n\lambda}\cos(n\lambda\theta) + \sum_{n\in\mathbb{N}^*} \mathsf{a}_n^{i+n}\rho^{-n\lambda} cos(n\lambda\theta). \tag{26}$$

The field $\ln(\rho)$ as well as the fields $\rho^{n\lambda}\cos(n\lambda\theta)$, for $n \geq 0$, are singular in Ω^∞ in the sense of Definition 1 (even the constant field 1 corresponding to $n = 0$ is singular). Since the fields $\rho^{-n\lambda}\cos(n\lambda\theta)$ are regular when $n \geq 1$, v^i is split into its singular and regular part as follows:

$$v^i(\mathbf{y}) = v^i_S(\mathbf{y}) + \bar{v}^i(\mathbf{y}), \tag{27}$$

$$v^i_S(\mathbf{y}) = \mathsf{a}^i_0 \ln(\rho) + \sum_{n=0}^{i} \mathsf{b}^i_n \rho^{n\lambda}\cos(n\lambda\theta), \quad \nabla\bar{v}^i \in L^2(\Omega^\infty), \quad \lim_{|\mathbf{y}|\to\infty} \bar{v}^i(\mathbf{y}) = 0. \tag{28}$$

Remark 3. *This analysis of the singularities shows that the singular parts of the fields u^i and v^i will be known once the coefficients a^i_n and b^i_n are determined for $0 \leq n \leq i$.*

2.2.5. *The problems defining the regular parts $\bar{u}^i$ and $\bar{v}^i$.* The singular parts (u^i_S, v^i_S) are harmonic, and satisfy the homogeneous Neumann boundary conditions on the edges of the notch. Therefore the regular parts are harmonic too, with data expressed in terms of the singular fields.

The first outer problem, $i = 0$
Find $\bar{u}^0$ regular in Ω_0 such that

$$\begin{cases} \Delta\bar{u}^0 = 0 & \text{in } \Omega^0 \\ \dfrac{\partial\bar{u}^0}{\partial\nu} = 0 & \text{on } \Gamma^+ \cup \Gamma^- \\ \dfrac{\partial\bar{u}^0}{\partial\nu} = h - \dfrac{\partial u^0_S}{\partial\nu} & \text{on } \Gamma_N \\ \bar{u}^0 = f - u^0_S & \text{on } \Gamma_D \end{cases} \tag{29}$$

The other outer problems, $i \geq 1$
Find $\bar{u}^i$ regular in Ω_0 such that

$$\begin{cases} \Delta\bar{u}^i = 0 & \text{in } \Omega^0 \\ \dfrac{\partial\bar{u}^i}{\partial\nu} = 0 & \text{on } \Gamma^+ \cup \Gamma^- \\ \dfrac{\partial\bar{u}^i}{\partial\nu} = -\dfrac{\partial u^i_S}{\partial\nu} & \text{on } \Gamma_N \\ \bar{u}^i = -u^i_S & \text{on } \Gamma_D \end{cases} \tag{30}$$

The first inner problem, $i = 0$
Find $\bar{v}^0$ regular in Ω^∞ such that

$$\begin{cases} \Delta\bar{v}^0 = 0 & \text{in } \Omega^\infty \\ \dfrac{\partial\bar{v}^0}{\partial\nu} = 0 & \text{on } \Gamma^+ \cup \Gamma^- \\ \dfrac{\partial\bar{v}^0}{\partial\nu} = g - \dfrac{\partial v^0_S}{\partial\nu} & \text{on } \Gamma_1 \end{cases} \tag{31}$$

The other inner problems, $i \geq 1$
Find $\bar{v}^i$ regular in Ω^∞ such that

$$\begin{cases} \Delta\bar{v}^i = 0 & \text{in } \Omega^\infty \\ \dfrac{\partial\bar{v}^i}{\partial\nu} = 0 & \text{on } \Gamma^+ \cup \Gamma^- \\ \dfrac{\partial\bar{v}^i}{\partial\nu} = -\dfrac{\partial v^i_S}{\partial\nu} & \text{on } \Gamma_1 \end{cases} \tag{32}$$

Consider first the outer problems. The well-posedness is a direct consequence of classical results for the Laplace equation:

Proposition 2. *Let $i \geq 0$. For a given singular part u^i_S, i.e. if the coefficients a^i_n are known for all n such that $0 \leq n \leq i$, then there exists a unique solution $\bar{u}^i$ of (30) (or of (29) when $i = 0$). Consequently, the coefficients b^{i+n}_n are then determined for all $n \geq 0$.*

As for the inner problems, since they are Neumann problems (except for the condition at infinity), defined in an infinite domain, more care must be taken. The well-posedness is ensured by a compatibility condition, as stated in Proposition 3.

Proposition 3. *Let $i \geq 0$. For given b^i_n with $0 \leq n \leq i$, there exists a regular solution $\bar{v}^i$ for the i-th inner problem if and only is the coefficient a^i_0 is such that*

$$\mathsf{a}^0_0 = -\frac{1}{\omega}\int_{\Gamma_1} g(s)ds, \qquad \mathsf{a}^i_0 = 0 \quad \textit{for} \quad i \geq 1. \tag{33}$$

Moreover, if this condition is satisfied, then the solution is unique and therefore the coefficients a^{i+n}_n are determined for all $n \geq 0$.

PROOF. The inner problems are pure Neumann problems in which no Dirichlet boundary conditions are imposed to the v^i except for the condition at infinity. Consequently, they admit a solution (if and) only if the Neumann data satisfy a global compatibility condition. Let us re-establish that condition. Let Ω^R be the part of Ω^∞ included in the ball of radius $R>1$, *i.e.* $\Omega^R=\Omega^\infty\cap\{\mathbf{y}:|\mathbf{y}|<R\}$. Consider first the case $i=0$. Integrating the equation $\Delta v^0=0$ over Ω^R and using the boundary conditions leads to

$$0=\int_{\partial\Omega^R}\frac{\partial v^0}{\partial\nu}ds=\int_0^\omega\frac{\partial v^0}{\partial\rho}(R,\theta)R\,d\theta+\int_{\Gamma_1}g(s)ds. \tag{34}$$

Using (26) yields $R\dfrac{\partial v^0}{\partial\rho}(R,\theta)=\mathsf{a}_0^0+\sum_{n\in\mathbb{N}^*}n\lambda\big(-\mathsf{c}_n^0R^{-n\lambda}+\mathsf{b}_n^0R^{n\lambda}\big)\cos(n\lambda\theta)$. Since $\int_0^\omega\cos(n\lambda\theta)d\theta=0$ for all $n\geq1$, after inserting in (34), the desired condition for a_0^0 appears. For $i\geq1$, the same process is applied, and the integral over Γ_1 vanishes, yielding the desired condition.

If the compatibility condition (33) is satisfied, then the existence of a regular solution for $\bar v^i$ is obtained by standard arguments. Note however that, since $\nabla\bar v^i$ belongs to $L^2(\Omega^\infty)$, $\bar v^i$ tends to a constant at infinity and this constant is fixed to 0 by the additional regularity condition. As far as the uniqueness is concerned, the solution of this pure Neumann problem is unique up to a constant and the constant is fixed by the condition that $\bar v^i$ vanishes at infinity.

Once v^i is determined, the coefficients a_n^{i+n} are obtained by virtue of Proposition 1 and (26). □

Remark 4. *If the forces applied to the boundary of the defect are equilibrated, i.e. if* $\int_{\Gamma_1}g(s)ds=0$, *then all the coefficients* a_0^i *vanish and hence the terms in* $\ln(\ell)$ *disappear in the inner expansion. There is no more logarithmic singularities in the* u^i *and the* v^i.

2.2.6. *The construction of the outer and inner expansions.* Recall the relationship between the coefficients $(\mathsf{a}_n^j,\mathsf{b}_n^j)$ and the singular and regular parts of the u_j and v_j.

$$\begin{array}{lll} u^j=u_S^j+\bar u^j, & u_S^j\longleftrightarrow(\mathsf{a}_n^j)_{n=0}^j, & \bar u^j\longleftrightarrow(\mathsf{b}_n^{j+n})_{n\geq0},\\ v^j=v_S^j+\bar v^j, & v_S^j\longleftrightarrow(\mathsf{a}_0^j,\ (\mathsf{b}_n^j)_{n=0}^j), & \bar v^j\longleftrightarrow(\mathsf{a}_n^{j+n})_{n\geq0}.\end{array} \tag{35}$$

Coefficients a_0^j vanish all but a_0^0 given by (33).

The scheme of the algorithm is the following. Suppose $i\geq1$, and u^j and v^j are known for $1\leq j\leq i-1$. The order of operations at step i is the following:

(1) u_S^i is determined by $(\bar v^{i-n})_{1\leq n\leq i}$,
(2) $\bar u^i$ is determined by u_S^i,
(3) v_S^i is determined by $(\bar u^{i-n})_{0\leq n\leq i}$,
(4) $\bar v^i$ is determined by v_S^i.

Details are given below.

Initialization

S1 Define a_0^0 by (33) , and hence u_S^0 by (22).
S2 From u_S^0, define $\bar u^0$ by (29), and hence $u^0=u_S^0+\bar u^0$ is determined.
S3 Define b_n^n for $n\geq0$ from (20) as the coefficients of $\bar u^0$, see the next subsection for the practical method. Hence, $v_S^0=\mathsf{a}_0^0+\mathsf{b}_0^0\ln(\rho)$ is determined from (28) .
S4 From v_S^0, $\bar v^0$ is computed by (31), and hence $v^0=v_S^0+\bar v^0$ is determined.
S5 Define a_n^n for $n\geq1$ from (26) as the coefficients of $\bar v^0$, see the next subsection for the practical method.

For $i \geq 1$, suppose that u^j and v^j have been determined, together with the coefficients in (35), for $0 \leq j \leq i-1$.

- R1 Since $\mathsf{a}_0^i = 0$, and writing for $1 \leq n \leq i$, $\mathsf{a}_n^i = \mathsf{a}_n^{(i-n)+n}$, u_S^i is given by (25), where the coefficients are determined by those of the $\bar{v}^j$ for $1 \leq j \leq i-1$.
- R2 $\bar{u}^i$ is obtained by solving (30).
- R3 The coefficients b_n^{i+n} for $n \geq 0$ are extracted from $\bar{u}^i$ in (23,24), see the next subsection for the practical method.
- R4 Since $\mathsf{a}_0^i = 0$, and using $\mathsf{b}_n^i = \mathsf{b}_n^{j+n}$ with $j = i-n$, v_S^i is determined from (28).
- R5 $\bar{v}^i$ is obtained by solving (32).
- R6 u^i and v^i are obtained by summing the singular and regular parts.

This iterative method is summarized in Table 2.

a_n^i / b_n^i	i=0	i=1	i=2	i=3	i=4
n=0	(33) /Outer 0	0 / Outer 1	0 / Outer 2	0 / Outer 3	0 / Outer 4
n=1	0	Inner 0 / Outer 0	Inner 1 / Outer 1	Inner 2 / Outer 2	Inner 3 / Outer 3
n=2	0	0	Inner 0 / Outer 0	Inner 1/ Outer 1	Inner 2 / Outer 2
n=3	0	0	0	Inner 0 / Outer 0	Inner 1 / Outer 1
n=4	0	0	0	0	Inner 0 / Outer 0

TABLE 2. Summary of the inductive method to obtain the coefficients a_n^i and b_n^i: in the corresponding cell is indicated the problem which must be solved

2.2.7. *The practical method for determining the coefficients* a_n^i *and* b_n^i *for* $0 \leq n \leq i$. Throughout this section, $\mathcal{C}_r$ denotes the arc of circle of radius r starting on Γ^- and ending on Γ^+:

$$\mathcal{C}_r = \{(r,\theta) \ : \ 0 \leq \theta \leq \omega\}.$$

The coefficients a_n^i and b_n^i can be obtained by path integrals (which are path independent) as asserted in the following Proposition.

Proposition 4. *Let $i \geq 0$. Assume that $\bar{v}^i$ and $\bar{u}^i$ are known. Then*

(1) *For $n \geq 1$, a_n^{i+n} is given by the following path integral over $\mathcal{C}_\rho$,which is independent of ρ provided that $\rho > 1$:*

$$\mathsf{a}_n^{i+n} = \frac{2\rho^{n\lambda}}{\omega} \int_0^\omega \bar{v}^i(\rho,\theta)\cos(n\lambda\theta)d\theta. \tag{36}$$

(2) *For $n \geq 0$, b_n^{i+n} is given by the following path integral over $\mathcal{C}_r$, which is independent of r provided that $0 < r < r^*$:*

$$\mathsf{b}_0^i = \frac{1}{\omega}\int_0^\omega \bar{u}^i(r,\theta)d\theta, \qquad \mathsf{b}_n^{i+n} = \frac{2r^{-n\lambda}}{\omega}\int_0^\omega \bar{u}^i(r,\theta)\cos(n\lambda\theta)d\theta \quad \textit{for} \quad n \geq 1. \tag{37}$$

PROOF. The proofs are identical for the two families of coefficients and then only that concerning b_n^{i+n} will be given. By (23), $\bar{u}^i$ is given for $0 < r < r^*$ by

$$\bar{u}^i(r,\theta) = \sum_{p\in\mathbb{N}} \mathsf{b}_p^{i+p} r^{p\lambda}\cos(p\lambda\theta),$$

which is for fixed r the Fourier series of $\bar{u}^i(r,\cdot)$. Formulas (37) follow. □

2.3. **Verification in the case of a small cavity.** This subsection is devoted to the verification of the construction of the Matched Asymptotic Expansion presented in the previous subsections on an example where the exact solution is obtained in a closed form and hence can be directly expanded. Specifically, we consider a Laplace's problem posed in a domain which consists in an angular sector delimited by two arc of circles. The radius of the outer circle is equal to 1 while the radius of the inner circle is ℓ, see Figure 3. Thus,

$$\Omega_\ell = \{\mathbf{x} = r\cos\theta\mathbf{e}_1 + r\sin\theta\mathbf{e}_2 \ : \ r \in (\ell, 1),\ \theta \in (0, \omega)\}.$$

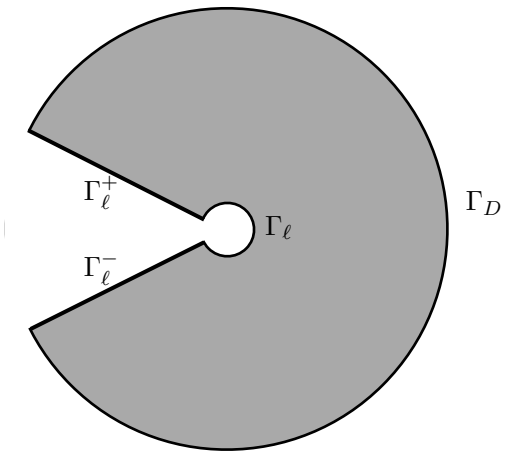

FIGURE 3. The domain Ω_ℓ in the case of a cavity

The sides of the notch and the inner circle are free and hence the boundary conditions on those parts of the boundary are

$$\frac{\partial u_\ell}{\partial \nu} = 0 \quad \text{on} \quad \Gamma_\ell^+ \cup \Gamma_\ell^- \cup \Gamma_\ell, \tag{38}$$

where $\Gamma_\ell^\pm = \{(r,\theta) : \ell < r < 1, \theta = 0 \text{ or } \omega\}$, $\Gamma_\ell = \{(r,\theta) : r = \ell, 0 \le \theta \le \omega\}$. (Note that $\Gamma_\ell^\pm$ depend on ℓ, contrarily to the assumption made in the remaining part of the paper. But that has no influence on the results.) The displacement is prescribed on the outer boundary Γ_D so that:

$$u_\ell(\mathbf{x}) = \cos\lambda\theta \quad \text{on} \quad \Gamma_D, \qquad \lambda = \frac{\pi}{\omega}. \tag{39}$$

Note that Γ_N is empty. Assuming that there is no body force, the exact solution of this anti-plane elastic problem is given by

$$u_\ell(\mathbf{x}) = \Big(\frac{\ell^{2\lambda}}{1+\ell^{2\lambda}} r^{-\lambda} + \frac{1}{1+\ell^{2\lambda}} r^{\lambda}\Big)\cos\lambda\theta. \tag{40}$$

Inserting the Taylor series of $1/(1+\ell^{2\lambda}) = \sum_{i\in\mathbb{N}}(-1)^i(\ell^{2\lambda})^i$ for $\ell < 1$, the expansion of u_ℓ at a given $\mathbf{x}$ takes the form:

$$u_\ell(\mathbf{x}) = r^\lambda\cos\lambda\theta + \sum_{n\in\mathbb{N}^*} \ell^{2n\lambda}(r^{-\lambda} - r^\lambda)\cos\lambda\theta. \tag{41}$$

Thus (41) corresponds to the outer expansion where the odd terms vanish and the even terms are given by

$$u^0(\mathbf{x}) = r^\lambda\cos\lambda\theta, \qquad u^{2n}(\mathbf{x}) = (-1)^n(r^\lambda - r^{-\lambda})\cos\lambda\theta, \quad \forall n \ge 1. \tag{42}$$

To obtain the inner expansion, replace r by $\ell\rho$ in (40), to get

$$u_\ell(\ell\mathbf{y}) = \frac{\ell^\lambda}{1+\ell^{2\lambda}}(\rho^{-\lambda} + \rho^\lambda)\cos\lambda\theta. \tag{43}$$

Inserting the Taylor series as before, the expansion of $u_\ell(\ell\mathbf{y})$ is given by

$$u_\ell(\ell\mathbf{y}) = \sum_{n\in\mathbb{N}} (-1)^n \ell^{(2n+1)\lambda} (\rho^{-\lambda} + \rho^\lambda) \cos\lambda\theta, \tag{44}$$

which corresponds to the inner expansion where the even terms vanish and the odd terms are given by

$$v^{2n+1}(\mathbf{y}) = (-1)^n (\rho^{-\lambda} + \rho^\lambda) \cos\lambda\theta, \quad \forall n \geq 0. \tag{45}$$

It remains to be checked that he procedure described in the previous subsections yields the same coefficients. Since $g = 0$, $\mathsf{a}_0^i = 0$ for all $i \geq 0$ and there is no logarithmic singularity, see Remark 4. The details for the first steps of the procedure are given below.

S1 By (33), $\mathsf{a}_0^0 = 0$ and hence $u_S^0 = 0$.
S2 Hence (29) becomes: $\Delta u^0 = 0$ in Ω_0, $\partial u^0/\partial\theta = 0$ on $\theta \in \{0, \omega\}$, $u^0 = \cos\lambda\theta$ on $r = 1$. The unique solution in $H^1(\Omega_0)$ is u^0 given by (42).
S3 By (37), $\mathsf{b}_1^1 = 1$ and $\mathsf{b}_n^n = 0$ for $n \neq 1$. Hence $v_S^0 = 0$.
S4 Since $v_S^0 = 0$ and $g = 0$, (31) gives $\bar{v}^0 = 0$ and hence $v^0 = 0$.
S5 By (36), $\mathsf{a}_n^n = 0$ for $n \geq 1$.
S6 By (25), $u_S^1 = 0$.
S7 By (30), $\bar{u}^1 = 0$ and hence $u^1 = 0$.
S8 By (37), $\mathsf{b}_n^{n+1} = 0$ for all n. Hence $v_S^1 = \rho^\lambda \cos\lambda\theta$.
S9 Hence (32) for $i = 1$ becomes: $\Delta\bar{v}^1 = 0$ in Ω^∞, $\partial\bar{v}^1/\partial\theta = 0$ on $\theta \in \{0, \omega\}$, $\partial\bar{v}^1/\partial\rho = -\lambda\cos\lambda\theta$ on $\rho = 1$. The unique regular solution is $\bar{v}^1 = \rho^\lambda\cos\lambda\theta$ and hence v^1 is given by (45).
S10 By (36), $\mathsf{a}_1^2 = 1$ and $\mathsf{a}_n^{n+1} = 0$ for $n \neq 1$.
S11 By (25), $u_S^2 = r^{-\lambda}\cos\lambda\theta$.
S12 Hence (30) for $i = 2$ becomes: $\Delta\bar{u}^2 = 0$ in Ω_0, $\partial\bar{u}^2/\partial\theta = 0$ on $\theta \in \{0, \omega\}$, $\bar{u}^2 = -\cos\lambda\theta$ on $r = 1$. The unique solution in $H^1(\Omega_0)$ is $\bar{u}^2 = -r^\lambda\cos\lambda\theta$ and hence u^2 is given by (42).
...

Proceeding by induction, the expected expansions are finally recovered . The end of the verification is left to the reader.

3. Application to the case of a crack

3.1. **Setting the problem.** In this section, the method is applied to a defect which is a non cohesive crack. Specifically, let Ω be the rectangle $(-H, L) \times (-H, +H)$. Let ϵ a given parameter in $(0, 1)$, $\mathcal{N} = \{\mathbf{x} = (x_1, x_2) : -H < x_1 \leq 0, |x_2| \leq \epsilon|x_1|)\}$. The notch-shaped body is $\Omega_0 = \Omega\backslash\mathcal{N}$. Finally the cracked body Ω_ℓ is obtained by removing from Ω_0 the line segment $\Gamma_\ell = (0, \ell)\times\{0\}$, see Figure 4.

The boundary Γ_D where the displacement is prescribed corresponds to the sides $D^\pm$ and D_L, with boundary conditions

$$u_\ell(\mathbf{x}) = \begin{cases} +H & \text{on} \quad D^+ = \{-H\}\times[\epsilon H, H], \\ -H & \text{on} \quad D^- = \{-H\}\times[-H, -\epsilon H], \\ 0 & \text{on} \quad D_L = \{L\}\times[-H, H]. \end{cases}$$

The remaining parts of the boundary (including the lips of the crack) are free, that is

$$\frac{\partial u_\ell}{\partial x_2} = \begin{cases} 0 & \text{on} \quad \Gamma_\ell = (0, \ell)\times\{0\} \\ 0 & \text{on} \quad N^\pm = (-H, L)\times\{\pm H\} \end{cases}$$

and

$$\frac{\partial u_\ell}{\partial n} = 0 \quad \text{on} \quad \Gamma^\pm = \{(x_1, x_2) : \ -H < x_1 < 0, \ x_2 = \pm \epsilon x_1\}.$$

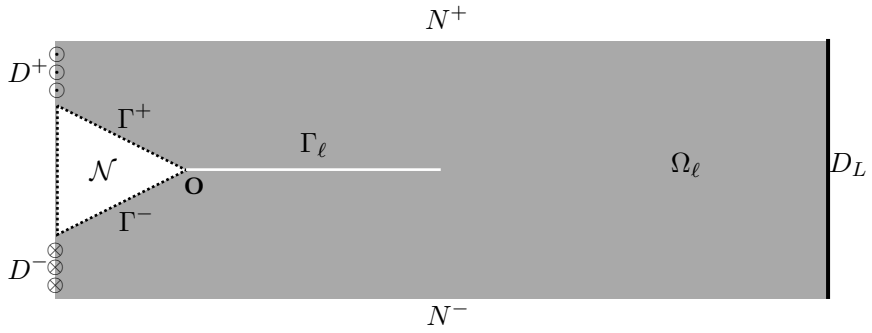

FIGURE 4. Definition of the cracked notch-shaped body Ω_ℓ with the various parts of the boundary.

Remark 5. *The amplitude of the prescribed displacement is normalized to H so that u_ℓ has the dimension of a length. The fact that the amplitude is equal to the height H has no importance in the present context of linearized elasticity. We will introduce a time dependent amplitude of the prescribed displacement when we study the propagation of the crack. Then the prescribed displacement will take "reasonable" values, controlled by the toughness of the material.*

Remark 6. *The case $\epsilon = 0$ corresponds to a body with an initial crack of length H and this limiting case is also considered in this paper. The case $\epsilon = 1$ corresponds to a corner with an angle $\pi/2$, the sides $D^\pm$ being reduced to the points $(-H, \pm H)$. This limiting case will not be considered here.*

Remark 7. *We only consider the case where the crack path is the line segment $(0, L)\times\{0\}$. It is a rather natural assumption by virtue of the symmetry of the geometry and the loading. An interesting extension should be to consider non symmetric geometry or loading and hence to take the direction of the crack as a parameter. This extension is reserved for future works.*

We are in the case where $g = 0$ on Γ_ℓ. Therefore, by virtue of Proposition 3, all the coefficients a_0^i vanish and there is no logarithmic singularities. Accordingly, the solution can be expanded as follows:

$$\textbf{Outer expansion} \quad u_\ell(\mathbf{x}) = u^0(\mathbf{x}) + \ell^\lambda u^1(\mathbf{x}) + \ell^{2\lambda} u^2(\mathbf{x}) + \ell^{3\lambda} u^3(\mathbf{x}) + \dots$$
$$\textbf{Inner expansion} \quad u_\ell(\mathbf{x}) = v^0(\mathbf{y}) + \ell^\lambda v^1(\mathbf{y}) + \ell^{2\lambda} v^2(\mathbf{y}) + \ell^{3\lambda} v^3(\mathbf{y}) + \dots$$

with

$$\lambda = \frac{\pi}{\omega} \qquad \text{and} \qquad \omega = 2\pi - 2\arctan(\epsilon). \tag{46}$$

By symmetry of the geometry and the loading, the real field u_ℓ is an odd function of x_2, *i.e.*

$$u_\ell(x_1, -x_2) = -u_\ell(x_1, x_2), \qquad u_\ell(r, \omega - \theta) = -u_\ell(r, \theta).$$

Therefore, all the fields u^i, $\bar{u}^i$, v^i, $\bar{v}^i$ admit the same symmetry. Therefore by Proposition 4, all coefficients b_{2n}^{i+2n} and a_{2n}^{i+2n} vanish. Consequently, the odd terms of the outer expansion and the

even terms of the inner expansions vanish, *i.e.* $u^{2i+1} = 0$ and $v^{2i} = 0$ for all $i \in \mathbb{N}$. Finally, the solution admits the following expansions:

$$\textbf{Outer expansion} \quad : \quad u_\ell(\mathbf{x}) = \sum_{i\in\mathbb{N}} \ell^{2i\lambda} u^{2i}(\mathbf{x}), \tag{47}$$

$$\textbf{Inner expansion} \quad : \quad u_\ell(\mathbf{x}) = \sum_{i\in\mathbb{N}} \ell^{(2i+1)\lambda} v^{2i+1}(\mathbf{y}). \tag{48}$$

By symmetry, the following coefficients vanish :

$$\mathsf{a}_n^i = 0 \quad \text{when } n \text{ or } i-n \text{ are even}, \qquad \mathsf{b}_n^i = 0 \quad \text{when } n \text{ is even or } i-n \text{ is odd}. \tag{49}$$

Examine now the singularities of ∇u_ℓ (in the sense that ∇u_ℓ is not bounded) according to whether or not$\ell = 0$, and according to whether or not$\epsilon = 0$.

(1) **When $\epsilon > 0$ and $\ell = 0$.** Then ∇u_0 is infinite at the tip of the notch and in its neighborhood has the form

$$\nabla u_0(\mathbf{x}) = \frac{\lambda \mathsf{b}_1^1}{r^{1-\lambda}} \Big(\cos(\lambda\theta)\mathbf{e}_r - \sin(\lambda\theta)\mathbf{e}_\theta \Big) + \text{regular terms}.$$

(2) **When $\epsilon > 0$ and $\ell > 0$.** Then ∇u_ℓ is no more infinite at the tip of the notch but becomes infinite at the tip of the crack, with the usual singularity in $1/\sqrt{r}$, see [8]. Specifically, ∇u_ℓ has the form

$$\nabla u_\ell(\mathbf{x}) = \frac{K_\ell}{\mu\sqrt{2\pi r'}} \Big(\sin\Big(\frac{\theta'}{2}\Big)\mathbf{e}_r + \cos\Big(\frac{\theta'}{2}\Big)\mathbf{e}_\theta \Big) + \text{regular terms}. \tag{50}$$

In (50) (r', θ') denotes the polar coordinate system such that $\mathbf{x} = (\ell + r'\cos\theta')\mathbf{e}_1 + r\sin\theta'\mathbf{e}_2$ and the angular function of θ' is normalized so that K_ℓ be the usual stress intensity factor. K_ℓ depends on ℓ and is "strongly" influenced by the presence of the notch when ℓ is small. (In fact, K_ℓ goes to 0 when ℓ goes to 0 as we will see below.) So, even if the stresses are only singular at the tip of the crack, there is a kind of overlapping of the previous singularity at the tip of the notch. This phenomenon renders the computations by the finite element method less accurate when ℓ is small.

(3) **When $\epsilon = 0$.** Then the notch is already a crack and it is unnecessary to treat separately $\ell = 0$ and $\ell > 0$. In any case ∇u_ℓ has the classical singularity in $1\sqrt{r}$ as in (50) and there is no more overlapping of two singularities. The computations by the finite element method are accurate in the full range of values of ℓ.

3.2. **The issue of the computation of the energy release rate.** The main goal of this section is to obtain accurate values for the *elastic energy* $\mathcal{P}_\ell$ stored in the cracked body and for its derivative with respect to ℓ, the so-called *energy release rate* $\mathcal{G}_\ell$, when ℓ is small. By definition, the elastic energy is given by

$$\mathcal{P}_\ell = \frac{1}{2}\int_{\Omega_\ell} \mu \nabla u_\ell \cdot \nabla u_\ell dx. \tag{51}$$

By virtue of Clapeyron's formula, the elastic energy stored in the body when the body is at equilibrium is equal to one half the work done by the external loads over the prescribed displacement on $D^\pm$. Therefore, using the symmetry of u_ℓ, the elastic energy can also be written as an integral over D^+:

$$\mathcal{P}_\ell = -\int_{\epsilon H}^{H} \mu H \frac{\partial u_\ell}{\partial x_1}(-H, x_2) dx_2, \tag{52}$$

which involves only the displacement field far from the tip of the notch.

By definition, see [7, 31], the *energy release rate* $\mathcal{G}_\ell$ is the opposite of the derivative of the elastic energy with respect to the length of the crack:

$$\mathcal{G}_\ell = -\frac{d\mathcal{P}_\ell}{d\ell}. \tag{53}$$

Even though $\mathcal{P}_\ell$ involves the ℓ dependent displacement field u_ℓ, its derivative does not involve the derivative $du_\ell/d\ell$ but can be expressed in terms of u_ℓ only. This property is a consequence of the fact that u_ℓ satisfies the equilibrium equations. Specifically, $\mathcal{G}_\ell$ can be computed either with the help of path integrals like the $\mathcal{J}$ integral of Rice [39] or by using the so-called $G-\theta$ method developed in [19]. We recall below the main ingredients of both methods when $0 < \ell < L$. The cases $\ell = 0$ and $\ell = L$ are treated separately.

In the former method, the integral $\mathcal{J}_\mathcal{C}$ over the path $\mathcal{C}$ is defined by

$$\mathcal{J}_\mathcal{C} = \int_\mathcal{C} \left(\frac{\mu}{2} \nabla u_\ell \cdot \nabla u_\ell n_1 - \mu \frac{\partial u_\ell}{\partial n} \frac{\partial u_\ell}{\partial x_1} \right) ds,$$

where $\mathbf{n}$ denotes the outer normal of the path. This integral is (theoretically) path-independent and equal to $\mathcal{G}_\ell$ provided that the path $\mathcal{C}$ starts from the lip of the crack, circumvents the tip of the crack and finishes on the lip of the crack like in Figure 5, see [8]. This path independency is used to obtain Irwin's formula [28, 31]. Indeed, taking for path the circle $\mathcal{C}_{r'}$ centered at the tip of the crack with radius r', using (50) and passing to the limit when $r' \to 0$, the following link between the energy release rate and the stress intensity factor K_ℓ introduced in (50) is obtained:

$$\mathcal{G}_\ell = \lim_{r' \to 0} \mathcal{J}_{\mathcal{C}_{r'}} = \frac{K_\ell^2}{2\mu}.$$

For the computations, the particularities of the geometry and of the loading can be exploited, to

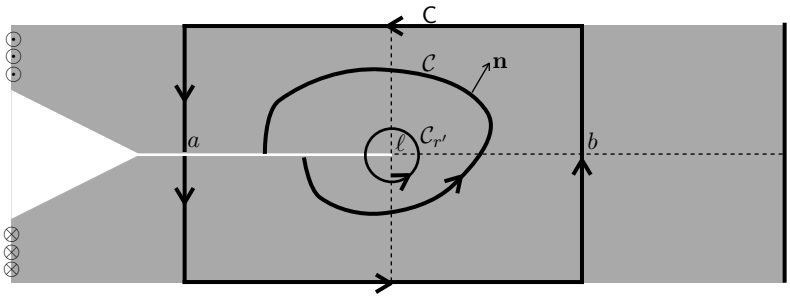

FIGURE 5. Examples of path for which $\mathcal{J}_\mathcal{C}$ is equal to $\mathcal{G}_\ell$.

choose a path made of line segments parallel to the axes like the path C in Figure 5:

$$\mathsf{C} = \{a\}\times(-H,0) \cup [a,b]\times\{-H\} \cup \{b\}\times(-H,H) \cup [a,b]\times\{+H\} \cup \{a\}\times(0,H) \quad \text{with} \quad 0 < a < \ell < b < L.$$

Then $\mathcal{J}_\mathsf{C} = \mathcal{G}_\ell$. Therefore, since $n_1 = 0$ and $\partial u_\ell/\partial n = 0$ on the sides $x_2 = \pm H$ and by virtue of the symmetry of u_ℓ, $\mathcal{G}_\ell$ takes the form

$$\mathcal{G}_\ell = \mu \int_{\{b\}\times(0,H)} \left(\left(\frac{\partial u_\ell}{\partial x_2}\right)^2 - \left(\frac{\partial u_\ell}{\partial x_1}\right)^2 \right) dx_2 - \mu \int_{\{a\}\times(0,H)} \left(\left(\frac{\partial u_\ell}{\partial x_2}\right)^2 - \left(\frac{\partial u_\ell}{\partial x_1}\right)^2 \right) dx_2. \tag{54}$$

From a theoretical point of view, a and b can be chosen arbitrarily, provided that they satisfy the constraints above. Indeed, the integral over the line segment $x_1 = a$ (resp. $(x_1 = b)$) does not depend on a (resp. on b) because u_ℓ is harmonic and satisfies homogeneous Neumann boundary conditions on $N^\pm$ and Γ_ℓ. (This verification is left to the reader, see [33, Proposition 8] for a proof.) However, from a numerical point of view, it is no more true because the computed displacement field does not satisfy exactly the equilibrium equations. Consequently, the computed values of $\mathcal{G}_\ell$

depend on the choice of a and b. Moreover, since the integral over the line a involves the gradient of the displacement, this integral can be badly approximated when ℓ is small because of the singularity.

The $G-\theta$ method is based on a change of variables which sends the ℓ-dependent domain Ω_ℓ onto a fix domain. In essence, it is the basic method to prove that $\ell \mapsto \mathcal{P}_\ell$ is differentiable, see [19] for the genesis of this method and [10] for a discussion on a generalization of the concept of energy release rate. In turn the $G-\theta$ approach gives a practical method to compute the energy release rate, see [10, 19]. Specifically, for a given $\ell > 0$, with a Lipschtiz continuous vector field $\boldsymbol{\theta}$ defined on Ω_ℓ, associate the following volume integral $\mathsf{G}_{\boldsymbol{\theta}}$:

$$\mathsf{G}_{\boldsymbol{\theta}} = \int_{\Omega_\ell} \left(\sum_{i,j=1}^{2} \mu \frac{\partial \theta_i}{\partial x_j} \frac{\partial u_\ell}{\partial x_i} \frac{\partial u_\ell}{\partial x_j} - \frac{\mu}{2} \nabla u_\ell \cdot \nabla u_\ell \ \mathrm{div}\boldsymbol{\theta} \right) dx.$$

It can shown that, if $\boldsymbol{\theta}$ is such that $\boldsymbol{\theta}(\ell, 0) = \mathbf{e}_1$ and $\boldsymbol{\theta} \cdot \mathbf{n} = 0$ on $\partial\Omega_\ell$, then $\mathsf{G}_{\boldsymbol{\theta}}$ is independent of $\boldsymbol{\theta}$ and equal to $\mathcal{G}_\ell$. Of course, this result of independency holds only when u_ℓ is the true displacement field. If it is numerically approximated, then $\mathsf{G}_{\boldsymbol{\theta}}$ becomes $\boldsymbol{\theta}$ dependent. In our case, owing to the simplicity of the geometry, we can use a very simple vector field $\boldsymbol{\theta}$ which renders the computations easier. Specifically, let $\boldsymbol{\theta}$ be given by

$$\boldsymbol{\theta}(\mathbf{x}) = \begin{cases} \mathbf{0} & \text{if } x_1 < 0, \\ \dfrac{x_1}{\ell}\mathbf{e}_1 & \text{if } 0 \le x_1 \le \ell, \\ \dfrac{L - x_1}{L - \ell}\mathbf{e}_1 & \text{if } \ell \le x_1 < L. \end{cases} \tag{55}$$

It satisfies the required conditions and hence $\mathsf{G}_{\boldsymbol{\theta}} = \mathcal{G}_\ell$. Accordingly, owing to the symmetry, $\mathcal{G}_\ell$ takes the form

$$\mathcal{G}_\ell = \frac{\mu}{L-\ell} \int_\ell^L \int_0^H \left(\Big(\frac{\partial u_\ell}{\partial x_2}\Big)^2 - \Big(\frac{\partial u_\ell}{\partial x_1}\Big)^2 \right) dx_2 dx_1 - \frac{\mu}{\ell} \int_0^\ell \int_0^H \left(\Big(\frac{\partial u_\ell}{\partial x_2}\Big)^2 - \Big(\frac{\partial u_\ell}{\partial x_1}\Big)^2 \right) dx_2 dx_1. \tag{56}$$

Comparing (56) with (54), (56) can be seen as an average of all the line integrals appearing in (54) when a and b vary respectively from 0 to ℓ and to ℓ and L. Accordingly, it can be expected that (56) gives more accurate computations than (54) when ℓ is small.

3.3. **Numerical results obtained for $\mathcal{G}_\ell$ by the FEM.** All the computations based on the finite element method are implemented into the industrial code COMSOL. They are performed after introducing dimensionless quantities. Specifically, in all the computations, the dimensions of the body are $H = 1$ and $L = 5$, the shear modulus $\mu = 1$. That does not restrict the generality of the study because the scale dependencies are known in advance. Indeed, the true physical quantities are related to the normalized quantities (denoted with a tilde) by

$$\ell = H\tilde{\ell}, \quad u_\ell = H\tilde{u}_\ell, \quad \mathcal{P}_\ell = \mu H^2 \tilde{\mathcal{P}}_\ell, \quad \mathcal{G}_\ell = \mu H \tilde{\mathcal{G}}_\ell. \tag{57}$$

For a given $\tilde{\ell} \in (0, 5)$ and a given $\epsilon \in (0, 1)$, we use the symmetry of the body and of the load to mesh only its upper half and prescribe $\tilde{u}_\ell = 0$ on the segment $\tilde{\ell} \le \tilde{x}_1 \le 5, \tilde{x}_2 = 0$. We use 6-nodes triangular elements, *i.e.* quadratic Lagrange interpolations. The mesh is refined near the singular corners and a typical mesh contains 25000 elements and 50000 degrees of freedom. We compute the discretized solution (still denoted) $\tilde{u}_\ell$ by solving the linear system. Then, the energy $\tilde{\mathcal{P}}_\ell$ and the energy release rate $\tilde{\mathcal{G}}_\ell$ are obtained by a post-processing. The energy is obtained by a direct integration of the elastic energy density over the body. The derivative of the energy is obtained by using formula (56), which needs to integrate the different parts of the elastic energy density over the two rectangles $(0, \tilde{\ell}) \times (0, 1)$ and $(\tilde{\ell}, 5) \times (0, 1)$. For a given ϵ, we compute $\tilde{\mathcal{P}}_\ell$ and $\tilde{\mathcal{G}}_\ell$ for $\tilde{\ell}$ varying from 0.001 to 5, first by steps of 0.001 in the interval $(0, 0.05)$, then by steps of 0.002 in the interval $(0.05, 0.2)$, finally by steps of 0.01 in the interval $(0.2, 5)$. The computations can

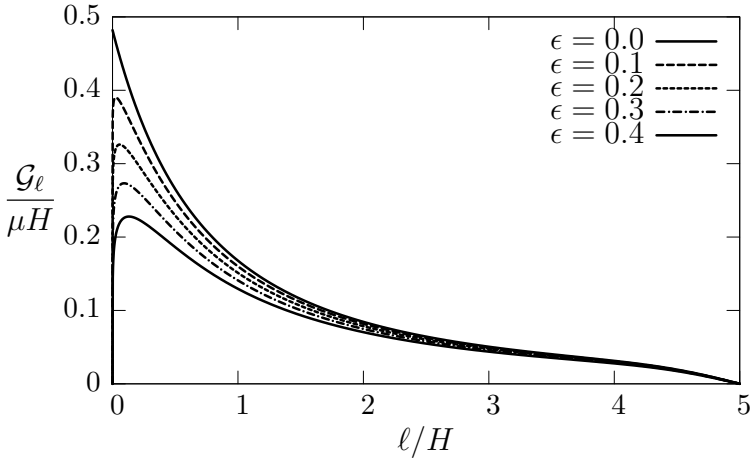

FIGURE 6. Computation by the Finite Element Method of the energy release rate $\mathcal{G}_\ell$ as a function of the crack length ℓ for five values of the notch angle.

be considered as sufficiently accurate for $\tilde{\ell} \geq 0.002$, even if this lower bound depends on ϵ, the computations being less accurate for small (but non-zero) values of ϵ. Below this value, if we try to refine the mesh near the corner of the notch, the results become mesh-sensitive, the linear system becomes ill-conditioned. Since only the part of the graph of $\tilde{\mathcal{G}}_\ell$ close to $\tilde{\ell} = 0$ is interesting when ϵ is small, we cannot obtain accurate results when ϵ is too small.(Of course, this remark does not apply when $\epsilon = 0$, because $\tilde{\ell} = 0$ is no more a "singular" case.)

The cases $\tilde{\ell} = 0$ and $\tilde{\ell} = 5$ with $\epsilon \neq 0$ are treated with specific meshes. We have only to compute $\tilde{u}_0$, $\tilde{\mathcal{P}}_0$, $\tilde{u}_L$ and $\tilde{\mathcal{P}}_L$, since $\tilde{\mathcal{G}}_0 = \tilde{\mathcal{G}}_L = 0$.

The case $\epsilon = 0$ is treated separately by adapting the previous methods. In particular, to calculate $\tilde{\mathcal{G}}_\ell$, the second integral in (56) is replaced by an integral over the rectangle $(-1, 0)\times(0, 1)$, and this integral is divided by $1+\tilde{\ell}$ instead of $\tilde{\ell}$. Moreover, the mesh is refined only near the tip of the crack, $\tilde{\ell} = 0$ is no more a particular case and the computations of $\tilde{\mathcal{G}}_\ell$ are accurate in the full range of $\tilde{\ell}$.

Let us highlight the main features of the numerical results plotted in Figure 6. These properties will be the basic assumptions from which we study the crack propagation at the end of the present section.

P1 For $\epsilon = 0$, $\mathcal{G}_\ell/\mu H$ is monotonically decreasing from 0.4820 to 0 when ℓ/H grows from 0 to 5.

P2 For $\epsilon > 0$, $\mathcal{G}_\ell/\mu H$ starts from 0 at $\ell/H = 0$, then is rapidly increasing. This growth is so important (for instance, $\mathcal{G}_\ell/\mu H = 0.1443$ when $\ell/H = 0.002$ for $\epsilon = 0.4$) that it cannot be correctly captured by the FEM.

P3 Still for $\epsilon > 0$, $\mathcal{G}_\ell$ is monotonically increasing as long as $\ell \leq \ell_{\mathsf{m}}$. At $\ell = \ell_{\mathsf{m}}$, $\mathcal{G}$ takes its maximal value G_{m}. Those values which depend on ϵ are given in the table below. It turns out that ℓ_{m}/H is rather small.

ϵ	0	0.1	0.2	0.3	0.4
ℓ_{m}/H	0	0.024	0.058	0.092	0.130
$\mathsf{G}_{\mathsf{m}}/\mu H$	0.4820	0.3900	0.3260	0.2733	0.2279

P4 For $\epsilon > 0$ again, $\mathcal{G}_\ell$ is monotonically decreasing from G_{m} to 0 when ℓ grows from ℓ_{m} to $5H$.

3.4. **Evaluation of the energy release rate by the MAM.** By virtue of (52), $\mathcal{P}_\ell$ can be expanded by using the outer expansion of u_ℓ. Using (47) leads to

$$\mathcal{P}_\ell = \sum_{i\in\mathbb{N}} P_{2i} \left(\frac{\ell}{H}\right)^{2i\lambda} \mu H^2, \tag{58}$$

where the coefficients P_{2i} of the expansions are dimensionless. The expansion of the energy release rate can be immediately deduce from that of the energy:

$$\mathcal{G}_\ell = -\sum_{i\in\mathbb{N}^*} 2i\lambda P_{2i} \left(\frac{\ell}{H}\right)^{2i\lambda-1} \mu H \tag{59}$$

and it is not necessary to use the path integrals $\mathcal{J}_\mathcal{C}$ or the $G-\theta$ method. Let us remark that

$$\mathcal{G}_0 = \begin{cases} 0 & \text{if } \epsilon \neq 0 \\ -P_2\mu H = K_0^2/2 > 0 & \text{if } \epsilon = 0 \end{cases} \tag{60}$$

because $\lambda > 1/2$ in the former case while $\lambda = 1/2$ in the latter.

To obtain the i^{th} term of the expansion of $\mathcal{P}_\ell$ and $\mathcal{G}_\ell$, both the singular part u_S^i and the regular part $\bar{u}^i$ of u^i must be recovered. The singular part involves the coefficients a_n^i for $1 \le n \le i$ which are obtained as the regular parts of the v^j for $j \le i$, see Section 2.2.6. Therefore, the inner problems must be solved, to determine the coefficients b_n^i for $0 \le n \le i$. In practise, these coefficients are obtained by using Proposition 4 after the inner and the outer problems have been solved with a finite element method. The advantage is that those problems do not contain a small defect and the accuracy is guaranteed. The drawback is that more and more problems have to be solved, in order to obtain accurate values of $\mathcal{G}_\ell$ when ℓ/H is not small.

ϵ	a_1^2	P_2	a_1^4	a_3^4	P_4	a_1^6	a_3^6	a_5^6	P_6
0	-0.3930	-0.4820	0.1888	0.0987	0.3282	-0.1365	-0.0537	-0.0494	-0.2013
0.1	-0.3756	-0.4413	0.1766	0.0943	0.3001	-0.1279	-0.0507	-0.0472	-0.1931
0.2	-0.3559	-0.3957	0.1619	0.0893	0.2673	-0.1165	-0.0470	-0.0446	-0.1787
0.3	-0.3342	-0.3486	0.1453	0.0838	0.2320	-0.1029	-0.0427	-0.0418	-0.1603
0.4	-0.3106	-0.3005	0.1273	0.0778	0.1952	-0.0880	-0.0380	-0.0389	-0.1385

TABLE 3. The computed values of the (non zero) coefficients a_n^i for $1 \le n \le i \le 6$ and of the leading terms P_2, P_4 and P_6 of the expansion of the potential energy for several values of the angle of the notch

ϵ	b_1^1	b_1^3	b_3^3	b_1^5	b_3^5	b_5^5
0	-0.7834	0.2384	-0.2059	-0.1943	0.1058	-0.0172
0.1	-0.7482	0.2091	-0.2085	-0.1730	0.0992	-0.0283
0.2	-0.7089	0.1777	-0.2081	-0.1489	0.0905	-0.0379
0.3	-0.6657	0.1451	-0.2045	-0.1232	0.0800	-0.0454
0.4	-0.6187	0.1125	-0.1977	-0.0974	0.0683	-0.0508

TABLE 4. The computed values of the (non-zero) coefficients b_n^i for $1 \le n \le i \le 5$ for several values of the angle of the notch

In the tables 3 and 4 are given the computed values of the first coefficients of the inner and outer expansions (still with $H = 1$, $L = 5$, $\mu = 1$). These tables contain all the terms which are necessary

to compute the expansions of the energy up to the sixth order, *i.e.* P_{2i} for $i \in \{0,1,2,3\}$. (Note that P_0 does not appear in the expansion of $\mathcal{G}_\ell$.) The graphs of $\ell \mapsto \mathcal{G}_\ell$ obtained from these expansions are plotted on Figure 7 in the cases $\epsilon = 0.2$ and $\epsilon = 0.4$. They are compared with the values obtained directly by the finite element code Comsol. From these comparisons, the following conclusions can be drawn:

- **C1** For very small values of ℓ, the first non trivial term (corresponding to $i = 1$ in (59)) of the Matched Asymptotic Expansion (denoted by MAM 2 on Figure 7) is sufficient to well approximate $\mathcal{G}_\ell$ while the FEM is unable to deliver accurate values.
- **C2** For values of ℓ of the order of ℓ_{m}, at least the first two non trivial terms (corresponding to $i = 1$ and 2 in (59)) of the MAE (denoted by MAM 4 on Figure 7), are necessary to capture the change of monotonicity of $\mathcal{G}_\ell$. Indeed, the first term being monotonically increasing is unable, alone, to capture that change of behavior.
- **C3** Still for values of ℓ of the order of ℓ_{m}, the first two terms are really sufficient to well approximate $\mathcal{G}_\ell$ provided that ℓ_{m}/H is sufficiently small. Specifically, the first two terms are sufficient as long as $\ell/H < 0.2$.
- **C4** Accordingly, the approximation of $\mathcal{G}_\ell$ by the first two non trivial terms of MAE can be used, in the range $[0, 2\ell_{\mathsf{m}}]$ of ℓ when $\epsilon \in (0, 0.4)$.
- **C5** As ℓ/H grows beyond 0.2, more and more terms of the MAE must be added, in order to get a good approximation of $\mathcal{G}_\ell$. Consequently, in the range of "large" values of ℓ/H, the direct FEM is accurate and hence is better to use.

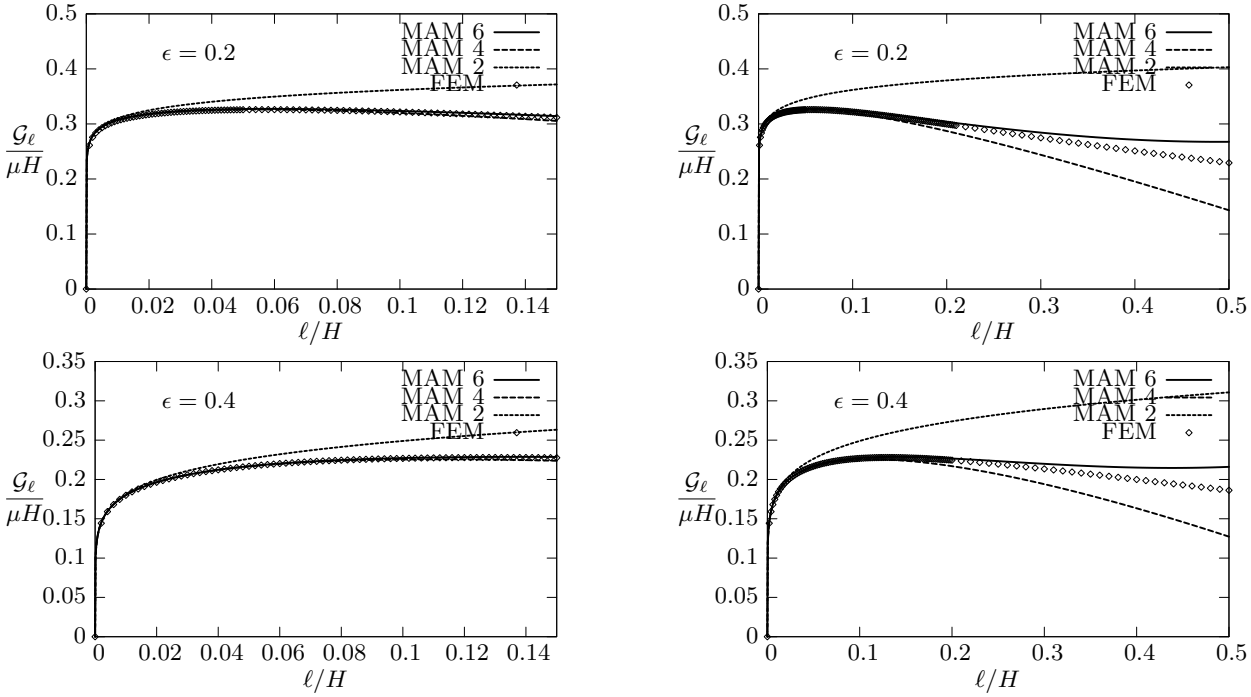

FIGURE 7. Comparisons of the graph of $\mathcal{G}_\ell$ obtained by the Matched Asymptotic Method or by the finite element code COMSOL in the cases $\epsilon = 0.2$ (above) and $\epsilon = 0.4$ (below). The diamonds correspond to the points obtained by FEM while the curves MAM $2i$, $i \in \{1,2,3\}$, correspond to the values obtained by considering the first i non trivial terms in the expansion of $\mathcal{G}_\ell$.

4. Application to the determination of the nucleation of the crack

The theoretical and numerical results obtained in the previous sections are used here to study the delicate issue of the nucleation of a crack in a sound body or the most classical question of the onset of a preexisting crack. Specifically, we consider the notched body Ω_0 which either contains a preexisting crack $\ell_0 > 0$ or is sound, *i.e.* $\ell_0 = 0$. We have also to distinguish different cases according to whether $\epsilon = 0$ or $\epsilon > 0$. The nucleation or the onset of cracking is governed by either the so-called *G-law* or the so-called *FM-law* and one goal of this section is to compare those laws. The interested reader can also refer to [7, 22, 36, 37, 33] where other comparisons between *G-law* and *FM-law* are proposed.

The notched body is submitted to a time-dependent loading process which consists in a monotonically increasing amplitude of the displacement prescribed on the sides $D^{\pm}$. Specifically, consider the new boundary conditions

$$u = \pm tH \quad \text{on} \quad D^{\pm}, \qquad t \geq 0. \tag{61}$$

the other remain unchanged. (Note that the "time" parameter t is dimensionless.) The evolution problem consists in finding the time evolution of the length of the crack, *i.e.* $t \mapsto \ell(t)$ for $t \geq 0$, under the initial condition $\ell(0) = \ell_0 \in [0, L)$. For that, we first remark that, for a given time $t \geq 0$ and a given crack length $\ell \in [0, L]$, the displacement field which equilibrates the body is

$$u(t, \ell) = t u_\ell, \tag{62}$$

where u_ℓ is the displacement field introduced in Section 3.1. Accordingly, the potential energy and the energy release rate at time t with a crack length ℓ can be expressed as

$$\mathcal{P}(t, \ell) = t^2 \mathcal{P}_\ell, \qquad \mathcal{G}(t, \ell) = t^2 \mathcal{G}_\ell, \tag{63}$$

where $\mathcal{P}_\ell$ and $\mathcal{G}_\ell$ are given by (51) and (53).

The two evolutions law are based on the crucial Griffith's assumption [25] concerning the surface energy associated with a crack. Specifically, assume that there exists a material constant $\mathsf{G_c} > 0$ such that the surface energy of the body with a crack of length ℓ is

$$\mathcal{S}(\ell) = \mathsf{G_c} \ell. \tag{64}$$

Accordingly, the total energy of the body at equilibrium at time t with a crack of length ℓ becomes

$$\mathcal{E}(t, \ell) := \mathcal{P}(t, \ell) + \mathcal{S}(\ell) = t^2 \mathcal{P}_\ell + \mathsf{G_c} \ell. \tag{65}$$

Throughout this section we assume that $\ell \mapsto \mathcal{P}_\ell$ is continuously differentiable and monotonically decreasing. Moreover, some monotonic properties of $\ell \mapsto \mathcal{G}_\ell$ will be added when necessary according to the analysis made in the previous sections.

4.1. The two evolution laws.

Let us briefly introduce the two evolution laws, the reader interested by the details should refer to [33]. The first one, called the *G-law*, is the usual Griffith law based on the critical potential energy release rate criterion, see [8, 31, 38]. In essence, this law only investigates smooth (*i.e.* at least continuous) evolutions of the crack length with the loading. It consists in the three following items:

Definition 2 (*G-law*). *Let $\ell_0 \in [0, L]$. A continuous function $t \mapsto \ell(t)$ is said satisfying (or solution of) the* G-law *in the interval $[t_0, t_1]$ with the initial condition $\ell(t_0) = \ell_0$, if the three following properties hold*

1. **Irreversibility:** *$t \mapsto \ell(t)$ is not decreasing;*
2. **Energy release rate criterion:** *$\mathcal{G}(t, \ell(t)) \leq \mathsf{G_c}, \quad \forall t \in [t_0, t_1]$;*
3. **Energy balance:** *$\ell(t)$ is increasing only if $\mathcal{G}(t, \ell(t)) = \mathsf{G_c}$, i.e. if $\mathcal{G}(t, \ell(t)) < \mathsf{G_c}$ at some t, then $\ell(t') = \ell(t)$ for every t' in a certain neighborhood $[t, t + h)$ of t.*

The third item implies that the release of potential energy is equal to the created surface energy when the crack propagates which justifies its name of energy balance. Consequently, if $t \mapsto \ell(t)$ is absolutely continuous, then the third item is equivalent to $\frac{\partial \mathcal{E}}{\partial \ell}(t, \ell(t))\dot{\ell}(t) = 0$ for almost all t and the following equality holds for almost all t:

$$\frac{d}{dt}\mathcal{E}(t, \ell(t)) = \frac{\partial \mathcal{E}}{\partial t}(t, \ell(t)). \tag{66}$$

A major drawback of the *G-law* is to be unable to take into account discontinuous crack evolutions, which renders it useless in many situations as we will see in the next subsection. It must be replaced by another law which admits discontinuous solutions. Another motivation of changing the *G-law* is to reinforce the second item by introducing a full stability criterion, see [22, 38, 7]. Specifically, let us consider the following local stability condition

$$\forall t \geq 0, \exists h(t) > 0 \quad : \quad \mathcal{E}(t, \ell(t)) \leq \mathcal{E}(t, l) \quad \forall l \in [\ell(t), \ell(t) + h(t)], \tag{67}$$

which requires that the total energy at t is a "unilateral" local minimum. (The qualifier unilateral is added because the irreversibility condition leads to compare the energy at t with only that corresponding to greater crack length, see [7]). Taking $l = \ell(t) + h$ with $h > 0$ in (67), dividing by h and passing to the limit when $h \to 0$, we recover the critical energy release rate criterion. Thus, the second item can be seen as a first order stability condition, weaker than (67). A stronger requirement consists in replacing local minimality by global minimality. It was the condition introduced by Francfort-Marigo in [22] in the spirit of the original Griffith idea [25] and that we will adopt here. Thus, the second evolution law, called *FM-law*, consists in the three following items

Definition 3 (*FM-law*)**.** *A function $t \mapsto \ell(t)$ (defined for $t \geq 0$ and with values in $[0, L]$) is said satisfying (or solution of) the* FM-law *if the three following properties hold*

1. **Irreversibility:** *$t \mapsto \ell(t)$ is not decreasing;*
2. **Global stability:** *$\mathcal{E}(t, \ell(t)) \leq \mathcal{E}(t, l), \quad \forall t \geq 0$ and $\forall l \in [\ell(t), L]$;*
3. **Energy balance:** *$\mathcal{E}(t, \ell(t)) = \mathcal{E}(0, \ell_0) + \int_0^t \frac{\partial \mathcal{E}}{\partial t'}(t', \ell(t'))\, dt', \quad \forall t \geq 0.$*

Let us note that the irreversibility condition is unchanged, while the energy balance condition is now written as the integrated form of (66), which does not require that $t \mapsto \ell(t)$ be continuous. Note also that the energy balance implies $\ell(0) = \ell_0$ because $0 = \mathcal{E}(0, \ell(0)) - \mathcal{E}(0, \ell_0) = \mathsf{G_c}(\ell(0) - \ell_0)$, and that the second item is automatically satisfied at $t = 0$ because $\mathcal{E}(0, l) = \mathsf{G_c} l$.

4.2. **The main properties of the *G-law* and the *FM-law*.** We recall or establish in this subsection some results for the two evolution laws under the assumptions of monotonicity of $\ell \mapsto \mathcal{G}_\ell$ resulting of the numerical computations, see **P1**–**P4** in Section 3.3. Some of those results have a general character and have been previously established in [7, 22, 33] while the other ones are specific to the present problem. In the case of properties which have already been obtained, we simply recall them without proofs.

Let us first consider the case when the notch is in fact a crack. Then, the two laws are equivalent by virtue of

Proposition 5. *In the case $\epsilon = 0$, since $\ell \mapsto \mathcal{G}_\ell$ is decreasing from $\mathcal{G}_0 > 0$ to 0 when ℓ goes from 0 to L (see Property* **P1***), the* G-law *and the* FM-law *admit the same and unique solution. Specifically, the preexisting crack begins to propagate at time $\mathsf{t_i}$ such that $\mathsf{t_i}^2 \mathcal{G}_{\ell_0} = \mathsf{G_c}$. Then the crack propagates continuously and $\ell(t)$ is such that $t^2 \mathcal{G}_{\ell(t)} = \mathsf{G_c}$. Since $\mathcal{G}_L = 0$, the crack will not reach the end L in a finite time.*

Proof. See [33, Proposition 18]. □

In the case of a guenuine notch, as far as the nucleation and the propagation of a crack with the *G-law* are concerned, we have

Proposition 6. *In the case $\epsilon > 0$, according to $\ell_0 = 0$ or $\ell_0 \in (0, \ell_\mathsf{m})$ or $\ell_0 \in [\ell_\mathsf{m}, L)$, the crack evolution predicted by the* G-law *is as follows*

(1) *If $\ell_0 = 0$, since $\mathcal{G}_0 = 0$, the unique solution to* G-law *is $\ell(t) = 0$ for all t, i.e.* **there is no crack nucleation***;*
(2) *If $\ell_0 \in (0, \ell_\mathsf{m})$, then the preexisting crack begins to propagate at time $\mathsf{t_i}$ such that ${\mathsf{t_i}}^2\mathcal{G}_{\ell_0} = \mathsf{G_c}$. But at $\mathsf{t_i}$* **the propagation is necessarily discontinuous** *and hence there is no continuous solution to* G-law *for $t \geq \mathsf{t_i}$;*
(3) *If $\ell_0 \in [\ell_\mathsf{m}, L)$, since $\ell \mapsto \mathcal{G}_\ell$ is monotonically decreasing in the interval (ℓ_m, L), the situation is the same as in Proposition 5. There exists a unique solution for the* G-law*: the crack begins to propagate at $\mathsf{t_i}$ (still given by ${\mathsf{t_i}}^2\mathcal{G}_{\ell_0} = \mathsf{G_c}$) and then propagates continuously until L which is reached asymptotically.*

Proof. Let us give the sketch of the proof for the first two items.

(1) Since $\ell_0 = 0$ and $\mathcal{G}_0 = 0$, then for all $t \geq 0$ one gets $0 = \mathcal{G}(t, 0) < \mathsf{G_c}$ and hence $\ell(t) = 0$ is a solution. The uniqueness follows from the initial condition and the energy balance.
(2) Since $0 < \ell_0 < \ell_\mathsf{m}$, then $\mathcal{G}_{\ell_0} > 0$ and hence $t^2\mathcal{G}_{\ell_0} = \mathcal{G}(t, \ell_0) \leq \mathsf{G_c}$ if and only if $t \in [0, \mathsf{t_i}]$. Since the inequality is strict when $t \in [0, \mathsf{t_i})$, then $\ell(t) = 0$ is the unique solution in this interval because of the initial condition and the energy balance. By continuity, it is also the unique solution in the closed interval $[0, \mathsf{t_i}]$. On the other hand, since $\mathcal{G}(t, \ell_0) > \mathsf{G_c}$ when $t > \mathsf{t_i}$, the crack must begin to propagate at $\mathsf{t_i}$.

   Let us show that no (continuous) evolution can satisfy the *G-law* for $t > \mathsf{t_i}$. Indeed, by construction $\mathcal{G}(\mathsf{t_i}, \ell(\mathsf{t_i})) = {\mathsf{t_i}}^2\mathcal{G}_{\ell_0} = \mathsf{G_c}$. But since $\ell(t) \geq \ell_\mathsf{i}$ for $t > \mathsf{t_i}$ and since $\ell \mapsto \mathcal{G}_\ell$ is monotonically increasing in the neighborhood of $\ell_0 < \ell_\mathsf{m}$, it holds for $t \in (\mathsf{t_i}, \mathsf{t_i} + h)$ and a sufficiently small $h > 0$:

$$\ell_0 < \ell(t) < \ell_\mathsf{m}, \qquad \mathcal{G}(t, \ell(t)) > \mathcal{G}(\mathsf{t_i}, \ell_0) = \mathsf{G_c}.$$

   Therefore the energy release rate criterion cannot be satisfied by a continuous evolution in a neighborhood of $\mathsf{t_i}$. The unique possibility is that the length of the crack jumps from ℓ_0 to some $\ell_\mathsf{i} > \ell_\mathsf{m}$ at time $\mathsf{t_i}$. But that requires to reformulate the *G-law*.

The proof of the third item is the same as in the previous Proposition and hence refers to [33, Proposition18]. □

Remark 8. *This property of no nucleation of a crack at a notch or of brutal propagation of a short crack is due to the fact that a notch with Neumann boundary conditions induces a* **weak singularity** *only, i.e. $\lambda > 1/2$. If one changes the boundary conditions by imposing the displacement on one edge of the notch and the stress on the other edge, then the singularity becomes* **strong** *for ω large enough and in such a case all the properties of nucleation are changed, see* [22, Proposition 4.19].

Consider now the *FM-law*. It is proved in [33, Proposition 3] that, in the case of a monotonically increasing loading, the *FM-law* is equivalent to a minimization problem of the total energy at each time, as precisely stated in the following Lemma

Lemma 7. *Let $\ell_0 \in [0, L)$ be the initial length of the crack. A function $t \mapsto \ell(t)$ satisfies the* FM-law *if and only if, at each t, $\ell(t)$ is a minimizer of $l \mapsto \mathcal{E}(t, l)$ over $[\ell_0, L]$. Therefore, the* FM-law *admits at least one solution and each solution grows from ℓ_0 to L.*

This property holds true for any $\epsilon \geq 0$. In the case $\epsilon > 0$ we can deduce precise results:

Proposition 8. *In the case $\epsilon > 0$, according to $\ell_0 \in [0, \ell_\mathsf{m})$ or $\ell_0 \in [\ell_\mathsf{m}, L)$, the crack evolution predicted by the* FM-law *is as follows*

(1) *If $\ell_0 \in [0, \ell_{\mathsf{m}})$, then the nucleation (if $\ell_0 = 0$) or the propagation of the preexisting crack (if $\ell_0 \neq 0$) starts at time $\mathsf{t}_{\mathsf{i}} > 0$ and at this time the crack length* **jumps** *instantaneously from ℓ_0 to ℓ_{i}. The length ℓ_{i} is the unique length in (ℓ_{m}, L) such that*

$$\int_{\ell_0}^{\ell_{\mathsf{i}}} \mathcal{G}_\ell d\ell = (\ell_{\mathsf{i}} - \ell_0)\mathcal{G}_{\ell_{\mathsf{i}}} \quad \textit{or equivalently} \quad \mathcal{P}_{\ell_0} - \mathcal{P}_{\ell_{\mathsf{i}}} = (\ell_{\mathsf{i}} - \ell_0)\mathcal{G}_{\ell_{\mathsf{i}}} \tag{68}$$

while the time t_{i} is given by

$$\mathsf{t}_{\mathsf{i}}{}^2 \mathcal{G}_{\ell_{\mathsf{i}}} = \mathsf{G}_{\mathsf{c}}. \tag{69}$$

After this jump, the crack propagates continuously from ℓ_{i} to L, the evolution satisfying then the G-law*, i.e.*

$$t^2 \mathcal{G}_{\ell(t)} = \mathsf{G}_{\mathsf{c}}, \quad \forall t > \mathsf{t}_{\mathsf{i}}.$$

(2) *If $\ell_0 \in [\ell_{\mathsf{m}}, L)$, since $\ell \mapsto \mathcal{G}_\ell$ is monotonically decreasing in the interval (ℓ_{m}, L), the situation is the same as in Proposition 5. There exists a unique solution for the* FM-law *which is the same as for the* G-law*: the crack begins to propagate at t_{i} such that $\mathsf{t}_{\mathsf{i}}{}^2 \mathcal{G}_{\ell_0} = \mathsf{G}_{\mathsf{c}}$ and then propagates continuously until L which is reached asymptotically.*

Remark 9. *Before the proof of this Proposition, let us comment and interpret the equation* (68) *giving the jump of the crack at t_{i}.*

- *Let us first prove that ℓ_{i} is well defined by* (68)*. Let $\ell \mapsto g(\ell)$ be the function defined for $\ell \in (\ell_{\mathsf{m}}, L)$ by*

$$g(\ell) = \int_{\ell_0}^{\ell} \mathcal{G}_l \, dl - (\ell - \ell_0)\mathcal{G}_\ell.$$

  Its derivative is given by $g'(\ell) = -(\ell - \ell_0)\mathcal{G}'_\ell$ and hence is positive because $\mathcal{G}_\ell$ is decreasing in (ℓ_{m}, L). Since $\mathcal{G}_\ell < \mathsf{G}_{\mathsf{m}} := \mathcal{G}_{\ell_{\mathsf{m}}}$, $g(\ell_{\mathsf{m}}) < 0$ whereas $g(L) > 0$ because $\mathcal{G}_L = 0$. Therefore, there exists a unique $\ell \in (\ell_{\mathsf{m}}, L)$ such that $g(\ell) = 0$, what is precisely the definition of ℓ_{i}.
- *The equation* (68) *giving ℓ_{i} has a graphical interpretation. Indeed, the integral over $(\ell_0, \ell_{\mathsf{i}})$ represents the area under the graph of $\ell \mapsto \mathcal{G}_\ell$ between the lengths ℓ_0 and ℓ_{i}. On the other hand the product $(\ell_{\mathsf{i}} - \ell_0)\mathcal{G}_{\ell_{\mathsf{i}}}$ represents the area of the rectangle whose height is $\mathsf{G}_{\mathsf{i}} := \mathcal{G}_{\ell_{\mathsf{i}}}$. Therefore, since these two areas are equal, the two gray areas of Figure 8 are also equal. This rule of equality of the areas determines ℓ_{i} and, by essence, the line $\mathcal{G} = \mathsf{G}_{\mathsf{i}}$ is the classical Maxwell line which appears in any problem of minimization of a non convex function.*

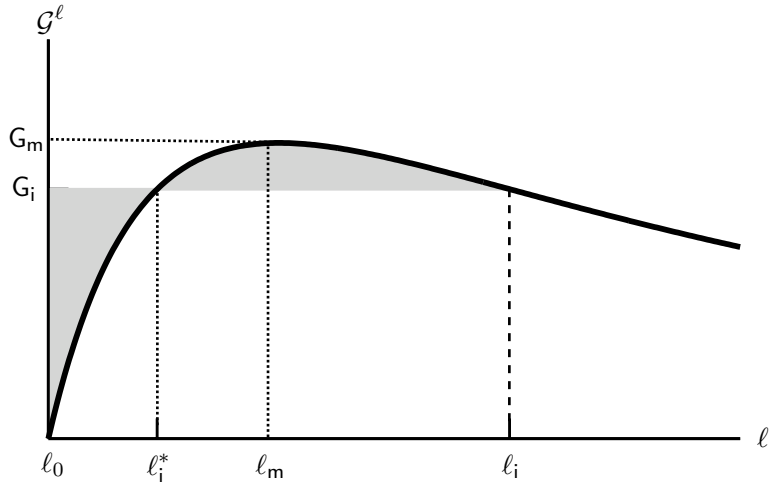

FIGURE 8. Graphical interpretation of the criterion of crack nucleation given by *FM-law* and which obeys to the Maxwell rule of equal areas.

- *Note that* ℓ_i **is independent of the toughness** $\mathsf{G_c}$ **and of the shear modulus** μ **of the material**. *It is a characteristic of the structure and merely depends on the geometry and the type of loading. Here, it depends on* ϵ, H *and* L. *For a given* ϵ *and a given ratio* L/H, ℓ_i *is proportional to* H, $\ell_\mathsf{i} = \tilde{\ell}_\mathsf{i} H$. *This property is a consequence of the Griffith assumption on the surface energy.*
- **The critical loading amplitude** $\mathsf{t_i}$ **depends on the toughness and on the size of the body**. *Since* $\mathcal{G}_{\ell_\mathsf{i}} = \tilde{\mathcal{G}}_{\ell_\mathsf{i}} \mu H$, $\mathsf{t_i}$ *varies like* $1/\sqrt{H}$. *This size effect is also a consequence of the Griffith assumption on the surface energy.*
- *By virtue of* (68) *and* (69), **the energy balance holds at time** $\mathsf{t_i}$ *even if the crack jumps at this time, i.e. the total energy of the body just before the jump is equal to the total energy just after. Indeed, those energies are respectively given by*

$$\mathcal{E}(\mathsf{t_i}-, \ell_0) = {\mathsf{t_i}}^2 \mathcal{P}_{\ell_0} + \mathsf{G_c}\ell_0, \qquad \mathcal{E}(\mathsf{t_i}+, \ell_\mathsf{i}) = {\mathsf{t_i}}^2 \mathcal{P}_{\ell_\mathsf{i}} + \mathsf{G_c}\ell_\mathsf{i}.$$

Using (68), (69) *and the equality* $\mathcal{P}_{\ell_0} - \mathcal{P}_{\ell_\mathsf{i}} = \int_{\ell_0}^{\ell_\mathsf{i}} \mathcal{G}_\ell d\ell$, *then* $\mathcal{E}(\mathsf{t_i}-, \ell_0) = \mathcal{E}(\mathsf{t_i}+, \ell_\mathsf{i})$.

PROOF OF PROPOSITION 8. We just prove the first part of the Proposition and the reader should refer to [33, Proposition 18] for the proof of the second part. Let $\ell_0 \in [0, \ell_\mathsf{m})$. By virtue of Lemma 7, $\ell(t)$ is a minimizer of $\ell \mapsto \mathcal{E}(t, \ell)$ over $[\ell_0, L]$. (The minimum exists because the energy is continuous and the interval is compact.) Let ℓ_i, $\mathsf{t_i}$ be given by (68)-(69), let $\mathsf{G_i} = \mathcal{G}_{\ell_\mathsf{i}}$ and let ℓ_i^* be the other length such that $\mathcal{G}_{\ell_\mathsf{i}^*} = \mathsf{G_i}$, see Figure 8. Let us first remark that the function $\ell \mapsto \bar{g}(\ell)$ defined on $[\ell_0, L]$ by

$$\bar{g}(\ell) := \mathsf{G_i}(\ell - \ell_0) - \big(\mathcal{P}_{\ell_0} - \mathcal{P}_\ell\big)$$

is non negative and vanishes only at ℓ_0 and ℓ_i. Indeed, its derivative is $\bar{g}'(\ell) = \mathsf{G_i} - \mathcal{G}_\ell$. Hence, $\bar{g}$ is first increasing from 0 when ℓ grows from ℓ_0 to ℓ_i^*, then decreasing to 0 when ℓ grows from ℓ_i^* to ℓ_i, and finally increasing again from 0 when ℓ grows from ℓ_i to L.

Let us show that ℓ_0 is the unique minimizer of the total energy when $t < \mathsf{t_i}$. From (68) and (69), we get for all $\ell \in [\ell_0, L]$ and all $t \le \mathsf{t_i}$:

$$\mathcal{E}(t, \ell) - \mathcal{E}(t, \ell_0) = -t^2(\mathcal{P}_{\ell_0} - \mathcal{P}_\ell) + \mathsf{G_c}(\ell - \ell_0) \ge t^2 \bar{g}(\ell) \ge 0.$$

Moreover, the inequalities above are equalities if and only if $\ell = \ell_0$ when $t < \mathsf{t_i}$ and the result follows. Using the same estimates, we can deduce that ℓ_0 and ℓ_i are the two minimizers of the total energy at $t = \mathsf{t_i}$.

Let us show now that the minimizer is in the open interval (ℓ_i, L) when $t > \mathsf{t_i}$. From (68) and (69), we get for all $\ell \in [\ell_0, \ell_\mathsf{i})$ and all $t > \mathsf{t_i}$:

$$\mathcal{E}(t,\ell) - \mathcal{E}(t,\ell_\mathsf{i}) = t^2(\mathcal{P}_\ell - \mathcal{P}_{\ell_\mathsf{i}}) - \mathsf{G_c}(\ell_\mathsf{i} - \ell) > \mathsf{t_i}^2\big(\mathcal{P}_\ell - \mathcal{P}_{\ell_\mathsf{i}} - \mathsf{G_i}(\ell_\mathsf{i} - \ell)\big) = \mathsf{t_i}^2\big(\bar{g}(\ell) - \bar{g}(\ell_\mathsf{i})\big) = \mathsf{t_i}^2\bar{g}(\ell) \geq 0.$$

Hence, the minimizer cannot be in $[\ell_0, \ell_\mathsf{i})$. Since the derivative of the total energy at $\ell = \ell_\mathsf{i}$ is equal to $\mathsf{G_c} - t^2\mathsf{G_i} < 0$, ℓ_i is not the minimizer. In the same manner, since the derivative of the total energy at $\ell = L$ is equal to $\mathsf{G_c} - t^2\mathcal{G}_L = \mathsf{G_c} > 0$, L cannot be the minimizer. Therefore, the minimizer is in the interval (ℓ_i, L) when $t > \mathsf{t_i}$. Hence, it must be such that the derivative of the total energy vanishes, which yields $t^2\mathcal{G}_{\ell(t)} = \mathsf{G_c}$. Since $\ell \mapsto \mathcal{G}_\ell$ is monotonically decreasing from $\mathsf{G_i}$ to 0 when ℓ goes from ℓ_i to L, there exists a unique $\ell(t) \in (\ell_\mathsf{i}, L)$ such that $\mathcal{G}_{\ell(t)} = \mathsf{G_c}/t^2 < \mathsf{G_i}$. The proof of the first part is complete. □

4.3. **Computation of the crack nucleation by the MAM.** Let us consider the cases where ϵ is sufficiently small in order that $\ell \mapsto \mathcal{G}_\ell$ be well approximated by the first two non trivial terms of its Matched Asymptotic Expansion for ℓ in the interval $[0, 2\ell_\mathsf{m}]$, see **C4**. Accordingly, we have

$$\frac{\mathcal{G}_\ell}{\mu H} \approx 2\lambda\,|P_2|\left(\frac{\ell}{H}\right)^{2\lambda-1} - 4\lambda\,|P_4|\left(\frac{\ell}{H}\right)^{4\lambda-1}, \tag{70}$$

using the fact that $P_2 < 0$ and $P_4 > 0$. Therefore, the length ℓ_m where $\mathcal{G}_\ell$ is maximal and the maximum $\mathsf{G_m}$ are approximated by

$$\frac{\ell_\mathsf{m}}{H} \approx \left(\frac{(2\lambda-1)\,|P_2|}{2(4\lambda-1)\,|P_4|}\right)^{\frac{1}{2\lambda}}, \qquad \frac{\mathsf{G_m}}{\mu H} \approx \frac{4\lambda^2\,|P_2|}{4\lambda-1}\left(\frac{(2\lambda-1)\,|P_2|}{2(4\lambda-1)\,|P_4|}\right)^{\frac{2\lambda-1}{2\lambda}}. \tag{71}$$

Comparing with the values obtained by the FEM (see **P3** and Table 5), it appears that the agreement is very good for the maximum $\mathsf{G_m}$, less good for ℓ_m. The reason is that the localization of ℓ_m by the FEM is quite imprecise because the graph of $\mathcal{G}_\ell$ is very flat near ℓ_m: for instance, for $\epsilon = 0.3$, $\mathcal{G}_\ell$ computed at $\tilde{\ell} = 0.092$ is equal to 0.27327 while it is equal to 0.27307 at $\tilde{\ell} = 0.082$, *i.e.* with a relative difference less than 10^{-4}.

One can see also in Table 5 that the contribution of the next term, *i.e.* MAM 6, is weak when ϵ is less than 0.2. Its influence, in particular on ℓ_i, can be no more neglected when $\epsilon \geq 0.3$. Note also that MAM 4 underestimates while MAM 6 overestimates the lengths ℓ_m and ℓ_i. This bounding property is due to the alternate change of sign of the coefficients P_{2i} with i. However, it is checked numerically only, we are not able to prove it.

ϵ	0	0.1	0.2	0.3	0.4
λ	0.5	0.5164	0.5335	0.5511	0.5689
ℓ_{m}/H by FEM	0	0.024	0.058	0.092	0.130
ℓ_{m}/H by MAM 4	0	0.0255	0.0533	0.0823	0.1124
ℓ_{m}/H by MAM 6	0	0.0267	0.0584	0.0953	0.1387
$\mathsf{G}_{\mathsf{m}}/\mu H$ by FEM	0.4820	0.3900	0.3260	0.2733	0.2279
$\mathsf{G}_{\mathsf{m}}/\mu H$ by MAM 4	0.4820	0.3917	0.3264	0.2724	0.2257
$\mathsf{G}_{\mathsf{m}}/\mu H$ by MAM 6	0.4820	0.3917	0.3274	0.2743	0.2287
ℓ_{i}/H by FEM	0	0.0517	0.1131	0.1814	0.2561
ℓ_{i}/H by MAM 4	0	0.0499	0.1020	0.1544	0.2067
ℓ_{i}/H by MAM 6	0	0.0530	0.1163	0.1923	0.2964
$\mathsf{G}_{\mathsf{i}}/\mu H$ by FEM	0.4820	0.3864	0.3195	0.2650	0.2188
$\mathsf{G}_{\mathsf{i}}/\mu H$ by MAM 4	0.4820	0.3877	0.3195	0.2635	0.2157
$\mathsf{G}_{\mathsf{i}}/\mu H$ by MAM 6	0.4820	0.3881	0.3208	0.2662	0.2201
$\mathsf{t}_{\mathsf{i}}/\mathsf{t}_{\mathsf{c}}$ by FEM	1.440	1.605	1.766	1.938	2.132
$\mathsf{t}_{\mathsf{i}}/\mathsf{t}_{\mathsf{c}}$ by MAM 4	1.440	1.606	1.769	1.916	2.153
$\mathsf{t}_{\mathsf{i}}/\mathsf{t}_{\mathsf{c}}$ by MAM 6	1.440	1.605	1.766	1.938	2.131

TABLE 5. Comparisons of the values of ℓ_{m}, G_{m}, ℓ_{i}, G_{i} and t_{i} obtained by the FEM with those obtained by MAM 4 and MAM 6.

Using MAM 4 to calculate the nucleation, we obtain the following result

Proposition 9. *In the case of a genuine notch $\epsilon > 0$,*

(1) *if the body does not contain a preexisting crack ($\ell_0 = 0$), then the time t_{i} at which the crack nucleates and the length ℓ_{i} of the nucleated crack at this time are approximated with the MAM 4 by*

$$\frac{\ell_{\mathsf{i}}}{H} \approx 2^{\frac{1}{2\lambda}} \frac{\ell_{\mathsf{m}}}{H} \approx \left(\frac{(2\lambda-1)\,|P_2|}{(4\lambda-1)\,|P_4|}\right)^{\frac{1}{2\lambda}}, \quad {\mathsf{t}_{\mathsf{i}}}^2 \approx \frac{1}{\lambda\ 2^{\frac{1}{2\lambda}}} \frac{\mathsf{G}_{\mathsf{c}}}{\mathsf{G}_{\mathsf{m}}} \approx \frac{{\mathsf{t}_{\mathsf{c}}}^2}{8\lambda^3} \left(\frac{4\lambda-1}{|P_2|}\right)^{2-\frac{1}{2\lambda}} \left(\frac{4P_4}{2\lambda-1}\right)^{1-\frac{1}{2\lambda}}, \tag{72}$$

where ${\mathsf{t}_{\mathsf{c}}}^2 = \mathsf{G}_{\mathsf{c}}/\mu H$;

(2) *if the body contains a preexisting crack of length ℓ_0 such that $0 < \ell_0 < \ell_{\mathsf{m}}$, then the length ℓ_{i} at which the crack jumps at the onset of the propagation is the unique solution greater than ℓ_{m} of*

$$0 = |P_2| \Big((2\lambda-1)\ell_{\mathsf{i}}^{2\lambda} - 2\lambda\ell_0\ell_{\mathsf{i}}^{2\lambda-1} + \ell_0^{2\lambda}\Big) H^{2\lambda} - P_4\Big((4\lambda-1)\ell_{\mathsf{i}}^{4\lambda} + 4\lambda\ell_0\ell_{\mathsf{i}}^{4\lambda-1} - \ell_0^{4\lambda}\Big), \tag{73}$$

while the time t_{i} at which the onset occurs is given by ${\mathsf{t}_{\mathsf{i}}}^2 = \mathsf{G}_{\mathsf{c}}/\mathcal{G}_{\ell_{\mathsf{i}}}$. Therefore, ℓ_{i} and t_{i} decrease from the values given by (72) to ℓ_{m} and $\sqrt{\mathsf{G}_{\mathsf{c}}/\mathsf{G}_{\mathsf{m}}}$ given by (71) when ℓ_0 runs from 0 to ℓ_{m}.

PROOF. When $\ell_0 = 0$, using MAM 4, then (68) becomes

$$0 = (2\lambda-1)\,|P_2| \left(\frac{\ell_{\mathsf{i}}}{H}\right)^{2\lambda} - (4\lambda-1)\,|P_4| \left(\frac{\ell_{\mathsf{i}}}{H}\right)^{4\lambda}.$$

Using (71), (72) can be deduced after some calculations left to the reader. In the same manner, (73) is a direct consequence of (68) and (70). The monotonicity of ℓ_{i} and t_{i} with respect to ℓ_0 is easily checked from the graphical interpretation of (73), see Figure 8. □

Therefore, since $1/2 < \lambda < 1$ for a genuine notch, the length of the nucleated crack ℓ_{i} is less than

$2\ell_{\mathsf{m}}$ while the critical time $\mathsf{t_i}$ is not greater than $2^{1/4}\sqrt{\mathsf{G_c}/\mathsf{G_m}}$. For very sharp notch, *i.e.* when ϵ is small, then $2\lambda \approx 1+\epsilon/\pi$ and

$$\ell_{\mathsf{i}} \approx \frac{\epsilon\,|P_2|}{\pi P_4} H, \quad {\mathsf{t_i}}^2 \approx \frac{\mathsf{G_c}}{|P_2|\,\mu H},$$

where $P_2 \approx -0.4820$ and $P_4 \approx 0.3282$. Therefore we recover the response associated with a crack when the notch angle tends to 2π. The *FM-law* delivers an evolution which depends continuously of the parameter ϵ, in contrast with the *G-law*.

As long as the dependence of $\mathsf{t_i}$ on ℓ_0 is concerned, it turns out that the *FM-law* predicts that the variation of $\mathsf{t_i}$ is small when ℓ_0 goes from 0 to ℓ_{m} as can be seen on Figure 9 for $\epsilon = 0.4$. Indeed, $\mathsf{t_i}/\mathsf{t_c}$ decreases from 2.153 to 2.105 when ℓ_0 varies from 0 to $\ell_{\mathsf{m}} = 0.112\,H$. That constitutes also a strong difference with the prediction of the *G-law* for which $\mathsf{t_i}$ goes to infinity when ℓ_0 goes to 0.

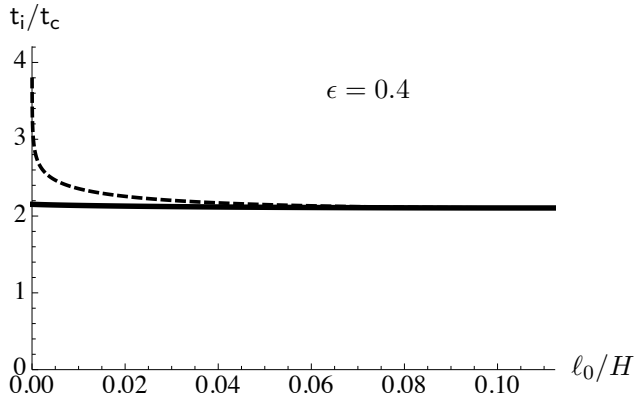

FIGURE 9. Time at which a preexisting crack starts in function of its length in the case where the notch parameter $\epsilon = 0.4$. Plain line: from the *FM-law*; dashed line: from the *G-law*

5. Conclusion and Perspectives

We have presented here a general method based on matched asymptotic expansions which can be applied to determine the mechanical fields and all related mechanical quantities in the case of a defect located at the tip of a notch. Applying this method to the case of a non cohesive crack, it turns out that it is sufficient to solve a few inner and outer problems to compute with a very good accuracy the dependency of the energy and the energy release rate on the length of the crack. Moreover, this approximation can be used for very small values of the length of the crack and hence to determine the onset of the cracking, whereas a classical finite element method gives rise to inaccurate results. In particular, the matched asymptotic method permits to compare the nucleation process of a crack at the tip of the notch which is predicted by the classical Griffith criterion with that predicted by the principle of energy minimization proposed in [22]. It turns out that the latter principle gives rise to much more relevant results than the former, from a physical viewpoint.

A natural extension of this work is to consider situations where the geometry and the loading have no symmetry and hence the direction that the nucleated crack will choose must also be predicted. Let us note that the *G-law* alone is not able to give an answer, and another criterion must be supplemented. In an anti-plane setting, the principle of local symmetry which is by essence made for an isotropic plane setting, cannot be used. It turns out that the *FM-law* in its general statement can also predict the direction and more generally the path of the crack, see [9, 10, 22]. So, an interesting challenge should be to use the MAM and the *FM-law* in a non symmetric case

to predict also the direction of nucleation. Another natural and desirable extension of the present work is to develop the method in a plane elasticity setting. It seems that there is no conceptual difficulty to do that. The last perspective concerns the choice of the surface energy. Indeed, the present study is based on the crucial Griffith assumption that the surface energy is proportional to the crack area. This assumption has very important consequences on the nucleation as we have seen in the paper. With this hypothesis, there is no cohesive force and hence the model does not contain the concept of critical stress. An important step will be to apply the MAM in the case of a cohesive crack [3, 20, 17] which automatically contains a critical stress and even a characteristic length. The goal will be to study the influence of those critical stress and characteristic length on the nucleation and the propagation of a crack in the spirit of the previous works based on the variational approach to fracture [2, 7, 12, 18, 21, 24, 29, 35].

References

[1] Abdelmoula, R. and J. J. Marigo: 2000, 'The effective behavior of a fiber bridged crack'. *J. Mech. Phys. Solids* **48**(11), 2419–2444.

[2] Abdelmoula, R., J.-J. Marigo, and T. Weller: 2010, 'Construction and justification of Paris-like fatigue laws from Dugdale-type cohesive models'. *Annals of Solid and Structural Mechanics* **1**(3-4), 139–158.

[3] Barenblatt, G. I.: 1962, 'The mathematical theory of equilibrium cracks in brittle fracture'. *Adv. Appl. Mech.* **7**, 55–129.

[4] Bilteryst, F. and J.-J. Marigo: 2003, 'An energy based analysis of the pull-out problem'. *Eur. J. Mech. A-Solid* **22**(1), 55–69.

[5] Bonnaillie-Noel, V., M. Dambrine, F. Herau, and G. Vial: 2010, 'On generalized Ventcel's type boundary conditions for Laplace operators in a bounded domain'. *SIAM J. Math. Anal.* **42**(2), 931–945.

[6] Bonnaillie-Noel, V., M. Dambrine, and G. Vial: 2011, 'Small Defects in Mechanics'. In: Simos, T E (ed.): *Internation Conference on Numerical Analysis and Applied Mathematics ICNAAM 2011, Vols A-C*. International Conference on Numerical Analysis and Applied Mathematics (ICNAAM), Halkidiki, Greece, September 19-25, 2011.

[7] Bourdin, B., G. A. Francfort, and J.-J. Marigo: 2008, 'The variational approach to fracture'. *J. Elasticity* **91**(1-3), 5–148.

[8] Bui, H. D.: 1978, *Mécanique de la rupture fragile*. Paris: Masson.

[9] Chambolle, A., G. A. Francfort, and J.-J. Marigo: 2009, 'When and how do cracks propagate?'. *J. Mech. Phys. Solids* **57**(9), 1614–1622.

[10] Chambolle, A., G. A. Francfort, and J.-J. Marigo: 2010, 'Revisiting energy release rates in brittle fracture'. *J. Nonlinear Sci.* **20**(4), 395–424.

[11] Chambolle, A., A. Giacomini, and M. Ponsiglione: 2008, 'Crack initiation in brittle materials'. *Arch. Ration. Mech. An.* **188**(2), 309–349.

[12] Charlotte, M., J. Laverne, and J.-J. Marigo: 2006, 'Initiation of cracks with cohesive force models: a variational approach'. *Eur. J. Mech. A-Solid* **25**(4), 649–669.

[13] Cherepanov, G. P.: 1979, *Mechanics of Brittle Fracture*. McGraw-Hill International Book Company.

[14] Dauge, M.: 1988, *Elliptic Boundary Value Problems in Corner Domains — Smoothness and Asymptotic of Solutions*, Lectures Notes in Mathematics. Springer Verlag.

[15] Dauge, M., S. Tordeux, and G. Vial: 2010, 'Selfsimilar perturbation near a corner: matching versus multiscale expansions for a model problem'. In: *Around the research of Vladimir Maz'ya. II*, Vol. 12 of *Int. Math. Ser. (N. Y.)*. Springer, pp. 95–134.

[16] David, M., J.-J. Marigo, and C. Pideri: 2012, 'Homogenized Interface Model Describing Inhomogeneities Localized on a Surface'. *J. Elasticity* **109**(2), 153–187.

[17] Del Piero, G. and M. Raous: 2010, 'A unified model for adhesive interfaces with damage, viscosity, and friction'. *Eur. J. Mech. A-Solid* **29**(4), 496–507.

[18] Del Piero, G. and L. Truskinovsky: 2009, 'Elastic bars with cohesive energy'. *Continuum Mech. Therm.* **21**(2), 141–171.

[19] Destuynder, P. and M. Djaoua: 1981, 'Sur une interprétation mathématique de l'intégrale de Rice en théorie de la rupture fragile'. *Math. Met. Appl. Sc* **3**, 70–87.

[20] Dugdale, D. S.: 1960, 'Yielding of steel sheets containing slits'. *J. Mech. Phys. Solids* **8**, 100–108.

[21] Ferdjani, H., R. Abdelmoula, and J.-J. Marigo: 2007, 'Insensitivity to small defects of the rupture of materials governed by the Dugdale model'. *Continuum Mech. Therm.* **19**(3-4), 191–210.

[22] Francfort, G. A. and J.-J. Marigo: 1998, 'Revisiting brittle fracture as an energy minimization problem'. *J. Mech. Phys. Solids* **46**(8), 1319–1342.
[23] Geymonat, G., F. Krasucki, S. Hendili, and M. Vidrascu: 2011, 'The matched asymptotic expansion for the computation of the effective behavior of an elastic structure with a thin layer of holes'. *Int. J. Multiscale Comput. Eng.* **9**(5), 529–542.
[24] Giacomini, A.: 2005, 'Size effects on quasi-static growth of cracks'. *SIAM J. Math. Anal.* **36**(6), 1887–1928.
[25] Griffith, A.: 1920, 'The phenomena of rupture and flow in solids'. *Phil. Trans. Roy. Soc. London* **CCXXI**(A), 163–198.
[26] Grisvard, P.: 1985, *Elliptic problems in non smooth domains*, No. 24 in Monographs and Studies in Mathematics. Pitman.
[27] Grisvard, P.: 1986, 'Problèmes aux limites dans les polygones; Mode d'emploi'. *EDF, Bulletin de la Direction des Études et Recherches* **Série C**(1), 21–59.
[28] Irwin, G. R.: 1958, 'Fracture'. *In Handlbuch des Physik, Springer Verlag* **6**, 551–590.
[29] Jaubert, A. and J.-J. Marigo: 2006, 'Justification of Paris-type Fatigue Laws from Cohesive Forces Model via a Variational Approach'. *Continuum Mech. Therm.* **V18**(1), 23–45.
[30] Lawn, B.: 1993, *Fracture of Brittle Solids - Second Edition*, Cambridge Solid State Science Series. Cambridge: Cambridge University press.
[31] Leblond, J.-B.: 2000, *Mécanique de la rupture fragile et ductile*, Collection Études en mécanique des matériaux et des structures. Editions Lavoisier.
[32] Leguillon, D.: 1990, 'Calcul du taux de restitution de l'énergie au voisinage d'une singularité'. *C. R. Acad. Sci. II b* **309**, 945–950.
[33] Marigo, J.-J.: 2010, 'Initiation of cracks in Griffith's theory: an argument of continuity in favor of global minimization'. *J. Nonlinear Sci.* **20**(6), 831–868.
[34] Marigo, J.-J. and C. Pideri: 2011, 'The effective behavior of elastic bodies containing microcracks or microholes localized on a surface'. *Int. J. Damage Mech.* **20**, 1151–1177.
[35] Marigo, J.-J. and L. Truskinovky: 2004, 'Initiation and propagation of fracture in the models of Griffith and Barenblatt'. *Continuum Mech. Therm.* **16**(4), 391–409.
[36] Negri, M.: 2008, 'A comparative analysis on variational models for quasi-static brittle crack propagation'. *Advances in Calculus of Variations* **3**(2), 149—212.
[37] Negri, M. and C. Ortner: 2008, 'Quasi-static crack propagation by Griffith's criterion'. *Math. Mod. Meth. Appl. S.* **18**, 1895–1925.
[38] Nguyen, Q. S.: 2000, *Stability and Nonlinear Solid Mechanics*. London: Wiley & Son.
[39] Rice, J. R.: 1968, 'A path independent integral and the approximate analysis of strain concentration by notches and cracks'. *J. Appl. Mech.* **35**, 379–386.
[40] Vidrascu, M., G. Geymonat, S. Hendili, and F. Krasucki: 2012, 'Matched asymptotic expansion and domain decomposition for an elastic structure'. In: *21st International Conference on Domain Decomposition Methods*. Rennes, France.

(T. B. T. Dang) Laboratoire de Mécanique des Solides, École Polytechnique, CNRS, UMR 7649, F-91128 Palaiseau cedex, France

E-mail address: tuyet@lms.polytechnique.fr

(L. Halpern) LAGA, Université Paris 13, Sorbonne Paris Cité, CNRS, UMR 7539, F-93430, Villetaneuse, France.

E-mail address: halpern@math.univ-paris13.fr

(J.-J. Marigo) Laboratoire de Mécanique des Solides, École Polytechnique, CNRS, UMR 7649, F-91128 Palaiseau cedex, France

E-mail address: marigo@lms.polytechnique.fr